



Combustion and emissions characteristics of toluene/n-heptane and 1-octene/n-octane binary mixtures in a direct injection compression ignition engine



Paul Hellier^{a,*}, Nicos Ladommatos^a, Robert Allan^b, John Rogerson^b

^a Department of Mechanical Engineering, University College London, Torrington Place, London WC1E 7JE, United Kingdom

^b BP Fuels and Lubricants Technology, BP Technology Centre, Whitchurch Hill, Pangbourne, Reading RG8 7QR, United Kingdom

ARTICLE INFO

Article history:

Received 22 November 2012
Received in revised form 25 March 2013
Accepted 24 April 2013
Available online 24 May 2013

Keywords:

Compression ignition combustion
Binary fuel mixtures
Emissions
Alkanes
Toluene
1-Octene

ABSTRACT

Successfully designing and making effective use of the next generation of liquid fuels, which will be derived from a range of biomass and fossil sources, requires an understanding of the interactions between structurally similar and dissimilar fuel components when utilised in current engine technology. Interactions between fuel components can influence the release of energy and production of harmful emissions in compression ignition combustion through determination of the autoignition behavior of the fuel. This paper presents experimental studies carried out in a single-cylinder engine supplied with a range of binary mixture fuels to investigate the effect of fuel component interactions on autoignition in direct injection compression ignition. A range of binary mixtures consisting of toluene and n-heptane and also 1-octene and n-octane were tested so as to observe respectively the effect of an aromatic compound and an alkene on n-alkane combustion and emissions. The engine tests were carried out at constant injection timing and they were repeated at constant ignition timing and at constant ignition delay, the latter being achieved through the addition to the various fuels of small quantities of ignition improver (2-ethylhexyl nitrate). Increasing the presence of toluene in the toluene/n-heptane binary mixtures resulted in an increased ignition delay time and generated a distinct two stage ignition process. An increased level of 1-octene in the binary mixtures of 1-octene/n-octane was also found to increase ignition delay, though to a much lesser extent than toluene in the case of the toluene/n-heptane mixtures. Interactions between the fuel components during the ignition delay period appear important in the case of the toluene/n-heptane mixtures but not those of 1-octene/n-octane. At constant injection and constant ignition timings, the combustion phasing and the level of emissions produced by each binary mixture were primarily driven by the ignition delay time. With ignition delay equalised, an effect of adiabatic flame temperature on NO_x production was visible.

© 2013 The Combustion Institute. Published by Elsevier Inc. Open access under [CC BY license](http://creativecommons.org/licenses/by/3.0/).

1. Introduction

There is consensus that anthropogenic release of CO₂ is resulting in global climate change [1], and this coupled with fears regarding security of supply of traditional fossil fuels is driving the move towards more sustainable future fuels. In addition, emissions legislation [2] reflects the need to reduce the levels of other environmentally harmful emissions from combustion of liquid fuels, such as NO_x [3] and particulate matter; optimising the efficiency of energy release, while decreasing pollutant emissions, will be key to the success of future fuels.

Such fuels will likely come from both refined fossil sources and biomass. In either case, the resulting fuel will be a mixture of many

compounds of dissimilar chemical structure. Manipulation of the composition of a fuel is already routinely used, for example in fossil diesel, to meet specifications regarding cold flow properties and cetane number. Varying proportions of fuel components has also been employed to better control homogeneous charge compression ignition (HCCI) combustion [4–6]. However, when designing a future fuel, a deeper understanding of how individual components are interacting to dictate combustion phasing and contributing to the production of emissions is invaluable.

Key to determining combustion phasing in compression ignition combustion is the ignition delay time exhibited by a fuel. Therefore, studying the autoignition properties of binary fuel mixtures has long been of interest in combustion research and, in particular, mixtures containing toluene have received much attention. As an aromatic compound, toluene is representative of the many such compounds found in fossil fuels, and of compounds produced

* Corresponding author.

E-mail addresses: p.hellier@ucl.ac.uk, hellier.pr@gmail.com (P. Hellier).

Nomenclature

NO _x	nitrogen oxides	SOC2	start of 2nd phase of combustion and point between SOC and the time of peak heat release rate at which $d(\tan^{-1}(dHRR/dCAD))$ is at a minimum and dHRR is positive
CO ₂	carbon dioxide	2 EHN	2 ethyl hexyl nitrate
IQT	ignition quality testing	CID	constant ignition delay
DCN	derived cetane number	IMEP	indicated mean effective pressure
CO	carbon monoxide	PPM	parts per million
THC	total hydrocarbons	FAME	fatty acid methyl ester
CAD	crank angle degree	HCCI	homogeneous charge compression ignition
PID	proportional integral derivative	RCM	rapid compression machine
DAQ	data acquisition	HRR	heat release rate
O ₂	oxygen	CFR	Cooperative Fuel Research
SOI	start of injection	SMD	Sauter mean diameter
BTDC	before top-dead-centre	CFD	computational fluid dynamics
TDC	top-dead-centre		
SOC	start of combustion		

from the catalytic cracking of crude renewable oils and the hydrothermal treatment of algal biomass [7,8]. Fuels suitable for compression ignition combustion nearly always require components that possess long alkyl chains in order to be of significant ignition quality, and several studies have investigated the interactions of toluene with n-heptane in differing proportions and at varying conditions.

Such investigations have in general focused on identifying the autoignition properties of toluene and n-heptane mixtures so as to further understanding of fuel effects on the phenomena of knock in SI engines and the rate of combustion in HCCI engines. One such means of doing so has been the rapid pressurisation of fuel and air mixtures in high pressure shock tubes. Herzler et al. [9] studied the ignition delay times of a mixture comprising 65% toluene and 35% n-heptane (by volume) at compression pressures of 10, 30 and 50 bar. While increasing the pressure consistently reduced ignition delay times, the effect of doing so became less important at higher pressures. For example, increasing the pressure from 10 to 30 bar resulted in a larger decrease in ignition delay than the same magnitude of pressure increase from 30 to 50 bar. Comparison of the data for the 65% toluene blend to that of pure n-heptane from a previous study [10] showed reduced negative temperature coefficient (NTC) reactivity for the toluene containing mixture. Hartman et al. [11] investigated the behavior of toluene and n-heptane blends containing up to 40% (volume) toluene in a high pressure shock tube at 40 bar and a temperature range of 700–1200 K. Above 20% toluene, further addition of toluene retarded the point of ignition and reduced the NTC region. Kinetic modelling suggested that the inhibiting effect of toluene on ignition of the mixtures to be highly temperature dependent and of greatest influence at 850 K for the conditions studied.

In studying HCCI in a rapid compression machine (RCM) with a peak compression ratio pressure of 4 bar, Tanaka et al. [4] observed the significantly longer ignition delay of a fully premixed blend comprising 74% toluene and 26% n-heptane compared to that of pure n-heptane. Andrae et al. [12] considered the autoignition of two toluene and n-heptane blends in a HCCI engine, both experimentally and through simulation. In engine tests, the blend containing a higher proportion of toluene exhibited longer ignition delays and initially the numerical simulation only accurately predicted these results when co-oxidation of the reactants was included. In addition to reactions involving the shared pool of radicals created by the oxidation of toluene and n-heptane, it

was suggested that reactions between the resulting benzyl and heptyl radicals were also important. However, a later refinement of the detailed model [13], utilising more accurate rate constants for the experimental conditions studied, found such reactions to be of less significance than originally considered.

Subsequently, Andrae et al. [14] in conducting semi-detailed kinetic modelling of toluene and n-heptane fuel mixtures, found the importance of cross reactions between the respective radicals of each fuel species to be dependent on the reaction conditions. In shock tube combustion at temperatures below 800 K, the inclusion of such reactions increased the model reactivity, but had no effect at higher temperatures or in HCCI simulations. Similarly, in conducting detailed kinetic modelling of surrogate gasoline fuels in a HCCI engine, Naik et al. [15] found that including cross reactions between the fuel components, which included toluene and n-heptane, had no effect on the model accuracy. Co-oxidation reactions between toluene and n-heptane were included in the modelling work of Anderlohr et al. [16], who found the reactivity of toluene to be influenced by the presence of NO_x, with hydrogen abstraction from toluene by NO₂ found to promote low temperature radical branching.

In a more recent RCM study, Di Sante [17] investigated the ignition delay times of a range of toluene and n-heptane mixtures in different proportions and at final compression temperatures. It was found that increasing the percentage of toluene present in the blend increased both the 1st and 2nd stage ignition delay times, though the influence of toluene addition diminished with increasing temperature.

Vanhove et al. [18] conducted a series of RCM experiments with a range of binary mixtures, including a 1/1 (% mols) toluene and n-heptane blend, at a range of temperatures between 650 and 900 K and a compression pressure of 3–5 bar. Analysis of the reaction mixtures during the ignition delay period revealed that in addition to n-heptane, toluene also underwent oxidation prior to autoignition. A similar mixture of benzene and n-heptane produced a similar profile of ignition delay with temperature, but sampling of the reaction mixture revealed that benzene had not reacted, suggesting that the inhibiting effect of toluene may not be chemical. Further mixtures of iso-octane and toluene did show a decrease in reactivity relative to pure iso-octane that was attributable to competition for radicals between the fuel components. This was attributed to the lesser reactivity of iso-octane relative to n-heptane, thus placing greater demand on the available radicals.

Xiao et al. [19] investigated the combustion and emissions production of binary mixtures of n-heptane and up to 20% (wt/wt) toluene in a Cooperative Fuel Research (CFR) indirect injection compression ignition engine. Increasing the percentage of toluene present in the blends increased the ignition delay time and also the levels of NO_x, THC and smoke emitted. An ignition improver (2 EHN) was subsequently added to the blend containing 20% toluene in increasing quantities until the blend displayed the same ignition delay time as pure n-heptane. With the effect of ignition delay removed, the presence of toluene did not see a significant increase in NO_x or THC levels, though an increase in smoke emissions remained. It was concluded that while the increase in NO_x and THC emissions with increasing toluene content could be attributed to the change in combustion phasing with increasing ignition delay, the increase in smoke emissions was independent of ignition delay and likely the result of the increasing blend aromatic ring content.

Alkenes are another prominent component of compression ignition fuels. Despite the similarity of alkenes and alkanes in that they both possess long alkyl chains which will dominate reactivity, there has been little direct study on the binary mixtures of such fuels (though the low temperature reactivity of alkenes as single components has been investigated [20–24]). Cullis et al. [25] investigated the ignition of n-heptane and 1-heptene mixtures in oxygen, and found that at below 600 K, 1-heptene did have an inhibiting effect on the reactivity of n-heptane. When considering a mixture of 1-hexene and iso-octane in the previously mentioned study [18], Vanhove et al. found no evidence of cross reactions between the two fuel components.

This paper presents results of experiments with a modern direct injection compression ignition engine in which binary mixtures of structurally dissimilar compounds, toluene/n-heptane, and structurally similar compounds, 1-octene/n-octane, were tested. This investigation therefore provides experimental results highlighting the effects of varying the proportions of two series of binary mixtures on combustion phasing and exhaust emissions, where the mixture components can be considered representative of current and potential future fuels.

2. Experimental methods

2.1. Apparatus

All combustion experiments presented were conducted in a single cylinder direct injection compression ignition engine specially

designed for combustion research. The binary fuel mixtures tested had physical properties, such as low lubricity, which would have resulted in damage to the fuel pump and common rail components. So, to overcome these issues, a previously designed and manufactured [26] low volume and high injection pressure fuel system was utilized.

Based on the concept first proposed and implemented by Schönborn et al. [27], the system uses the engine common rail system as a hydraulic fluid supply so as to pressurize a small quantity of the sample fuel (100–250 ml) via two free pistons. The redesigned system used for the tests discussed in this paper features a bypass operated by high pressure needle valves that allows fossil diesel fuel from the engine pump circuit to flow at pressure through the test fuel circuit. This allows the fuel system and combustion chamber to be flushed with a reference diesel between every test run. A schematic of the system is given in Fig. 1, with further details of the engine and control apparatus given in Table 1.

The engine cylinder gas pressure was measured and logged with a PC data acquisition system (National instruments) at every 0.2 CAD using a piezoelectric pressure transducer (Kistler 6056AU38) and charge amplifier (Kistler 5011). At bottom-dead-centre of every combustion cycle the cylinder pressure was pegged by the data acquisition system using a piezoresistive pressure transducer (Druck PTX 7517-3257) located in the intake manifold, 160 mm upstream of the inlet valves. The normally aspirated engine had a geometric compression ratio of 15.8:1. For all the tests air was aspirated into the combustion chamber at atmospheric pressure and temperature (30 °C). Various control and experiment temperatures were measured with K-type thermocouples and logged with the same PC data acquisition system utilized in recording in-cylinder pressures. The net apparent heat release rate was derived from the measured in-cylinder pressure during post-processing (MATLAB), as were the global gas temperatures utilizing a one dimensional and one zone thermodynamic model assuming homogeneity and ideal gas behavior of the cylinder contents.

Continuous exhaust gas sampling occurred 180 mm downstream of the exhaust valves to determine concentrations of gaseous species and also particulate size distribution. A gas analyzer system (Horiba MEXA 9100 HEGR) was supplied with sample gas via heated lines and was used to measure the following: NO_x concentrations by chemiluminescence; CO and CO₂ concentrations with non-dispersive infrared; paramagnetic analysis to determine O₂ concentrations; and levels of un-burnt hydrocarbons were measured with a flame ionization detector. Size and mass distributions

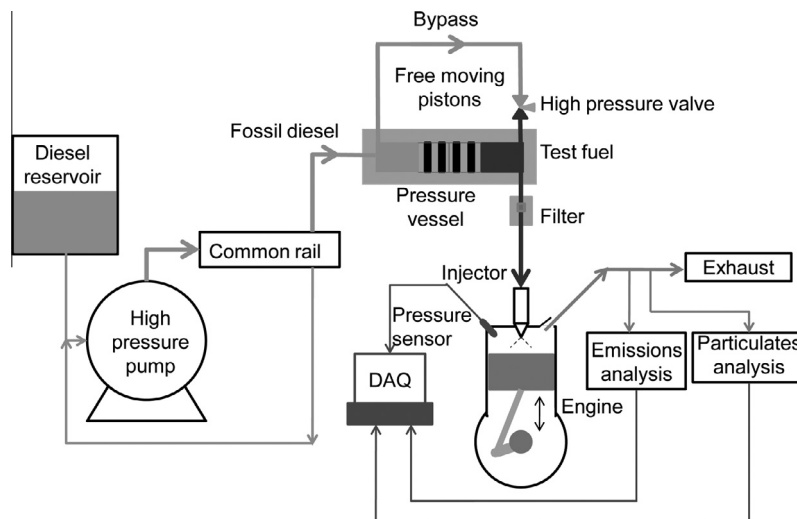


Fig. 1. Schematic showing operation of the low volume fuel system.

Table 1
Engine specification.

Engine head model	Ford Duratorq
Engine bottom end model	Ricardo Hydra
Number of cylinders	1
Cylinder bore	86 mm
Crankshaft stroke	86 mm
Swept volume	499.56 cc
Compression ratio	15.8:1
Maximum cylinder pressure	150 bar
Peak motoring pressure at test conditions	36 bar
Piston design	Central ω -bowl in piston
Oil temperature	80 \pm 2.5 °C
Water temperature	80 \pm 2.5 °C
Fuel injection pump	Single-cam radial-piston pump (BOSCH CP3)
High pressure fuel rail	Solenoid controlled, max. 1600 bar (BOSCH CRS2)
Injectors	6-hole solenoid controlled (DELPHI DFI 1.3)
Electronic fuel injection system	1 μ s resolution (EMTRONIX EC-GEN 500)
Shaft encoder	0.2 CAD resolution

of the sub-micron particles in the exhaust gas were determined by a differential mobility spectrometer (Cambustion DMS500). Sampling of exhaust gases for particulate measurements was made via a heated line, with a dilution cyclone located at the connection between the engine exhaust and heated line. Exhaust gases were diluted at this point by 4:1 and were diluted a second time upon entry to the analyser by 100:1. The sample line and both dilution cyclones were heated to a constant temperature of 75 °C.

2.2. Binary mixtures investigated

Binary mixtures comprising of two pairs of single molecules were tested in varying proportions to observe the following:

- The interaction of an aromatic compound with an n-alkane of equal carbon number.
- The interaction of a 1-alkene with an n-alkane of equal carbon number.

To investigate the interaction between an aromatic and n-alkane, toluene and n-heptane were selected. To observe the synergy between a 1-alkene and n-alkane, 1-octene and n-octane were chosen. All four of the pure component fuels were obtained from a chemical supplier (Sigma Aldrich). In addition, a fossil diesel fuel with zero FAME content was tested as a reference fuel. The assay and other properties of each fuel are presented in Table 2, while the molecular structure of each is given in Table 3.

2.3. Experimental conditions

Each of the binary mixtures and the reference diesel were initially tested at two experimental conditions: constant fuel injection timing and constant start of ignition timing. At constant injection timing the start of injection (SOI, defined as the time at which the injector actuating signal commences) was held constant at 7.5 CAD BTDC, and start of combustion for each fuel varied according to the ignition delay of that fuel. For constant ignition timing, the SOI was varied so that the SOC of all fuels always occurred at TDC. SOC was defined as the time in CAD (after SOI and before the time of peak heat release rate) at which the minimum value of cumulative heat release occurs.

In Fig. 2, heat release rate (HRR), cumulative heat release rate, the 1st derivative of heat release rate (dHRR) and $d(\tan^{-1}(dHRR/dCAD))$, where dCAD is the 1st derivative of crank angle position, are plotted against the crank angle position. Figure 2 also shows the definition of SOC in terms of cumulative heat release rate in the case of a binary mixture showing clear two stage combustion. The point at which the second stage of combustion commences (SOC2) is also displayed in Fig. 2. SOC2 is defined as the minimum

Table 2
Fuel properties.

	Molecular formula	Assay (%)	T_{boil} (°C)	T_{melt} (°C)	$\Delta v_{\text{H}}^{\circ}$ (kJ/mol)	Cetane number ²⁹	Density at 20 °C (kg/m ³)	Dynamic viscosity at 20 °C (mPa s)	Lower heating value (MJ/kg)
Reference fossil diesel	–	–	268.7 ^d	–	–	51.7 ^c	834.5 ^b	–	43.14 ^a
Toluene	C ₇ H ₈	99.8	111 [1]	–95.6 [2]	33.4 [3]	7.4 [4]	866.75 [5]	0.60 [5]	40.60 [6]
n-Heptane	C ₇ H ₁₆	99	98.4 [7]	–90.6 [8]	32.17[9]	54.4 [4]	684.06 [10]	0.41 [11]	44.50 [12]
1-Octene	C ₈ H ₁₆	98	121.3 [13]	–102.6 [13]	40.44 [14]	40.8 [4]	714.9 [15]	0.47 [15]	44.56 [16]
n-Octane	C ₈ H ₁₈	98	125.7 [17]	–56.9 [18]	41.53 [14]	64.1 [4]	702.8 [15]	0.546 [15]	44.79 [19]

[1] K. Aizawa, M. Kato, J. Chem. Eng. Data 36 (1991) 159–161.

[2] S.S.N. Murthy, Gangasharan, S.K. Nayak, J. Chem. Soc., Faraday Trans. 89 (1993) 509–514.

[3] G. Natarajan, D.S. Viswanath, J. Chem. Eng. Data 30 (1985) 137–140.

[4] M.J. Murphy, J.D. Taylor, R.L. McCormick, NREL/SR 540-36805 (2004).

[5] A.A. Silva, R.A. Reis, M.ü.L.L. Paredes, J. Chem. Eng. Data 54 (2009) 2067–2072.

[6] J.B. Heywood, Internal Combustion Engine Fundamentals, McGraw-Hill Book Company, 1988.

[7] C.H. Tu, H.Y. Hsian, Y.T. Chou, W.F. Wang, J. Chem. Eng. Data 46 (2001) 1239–1243.

[8] G.N. Brown, W.T. Ziegler, J. Chem. Eng. Data 24 (1979) 319–330.

[9] K.S. Pitzer, J. Am. Chem. Soc. 62 (1940) 1224–1227.

[10] E. Alonso, H. Guerrero, D. Montañó, C. Lafuente, H. Artigas, Thermochim. Acta 525 (2011) 71–77.

[11] E. Jimenez, C. Franjo, L. Segade, J.L. Legido, M.I.P. Andrade, J. Solution Chem. 27 (1998) 569–579.

[12] X. Lu, L. Ji, L. Zu, Y. Hou, C. Huang, Z. Huang, Combust. Flame 149 (2007) 261–270.

[13] A.L. Henne, K.W. Greenlee, J. Am. Chem. Soc. 65 (1943) 2020–2023.

[14] V. Majer, V. Svoboda, H.V. Kehiaian, International Union of Pure and Applied Chemistry, Enthalpies of Vaporization of Organic Compounds: A Critical Review and Data Compilation, Blackwell Scientific, Oxford, 1985.

[15] J.G. Speight, Lange's Handbook of Chemistry, McGraw-Hill, 2005.

[16] E.W. Prosen, F.D. Rossini, J. Res. Natl. Bureau Standards 38 (1945) 263–267.

[17] T. Hiaki, K. Takahashi, T. Tsuji, M. Hongo, K. Kojima, J. Chem. Eng. Data 40 (1995) 271–273.

[18] J. Bevan Ott, J. Rex Goates, J. Chem. Thermodynam. 15 (1983) 267–278.

[19] J.D. Rockenfeller, F.D. Rossini, J. Phys. Chem. 65 (1961) 267–272.

[20] Energy Institute (Institute of Petroleum), in: IP 12: Determination of Specific Energy, Energy Institute, 2001.

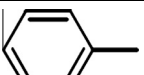



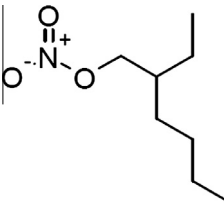
^a Calculated from experimental data obtained by the IP12 method [20].

^b Experimental data obtained according to ASTM D4052 at 15 °C.

^c Experimental data obtained according to EN ISO 516.

^d Point of 50% volume recovery obtained according to EN ISO 3405.

Table 3
Fuel and additive structures.

Toluene	
n-Heptane	
1-Octene	
n-Octane	
2 Ethylhexyl nitrate	

value of $d(\tan^{-1}(dHRR/dCAD))$ between SOC and the time of peak heat release rate where dHRR is positive.

After the initial two sets of experiments, at constant injection and constant ignition timing were completed, a third series of experiments was carried out during which the ignition delays of some of the different binary mixtures were held constant. This was achieved by adding the radical providing ignition improver (2 EHN, the molecular structure of which is given in Table 3) in small concentrations to each binary mixture, in an iterative process to determine the correct dosage to equal duration ignition delays. The experiments at constant ignition delay were conducted at both a fixed SOI of 7.5 CAD BTDC and also at a SOC of TDC. All of the binary mixtures treated with 2 EHN had ignition delays which differed, at most, only by the resolution of the engine shaft encoder (0.2 CAD).

All tests were conducted at an engine speed of 1200 rpm and at 450 bar fuel injection pressure. The injection duration was adjusted in the case of every fuel so that the engine IMEP was always constant at 4 bar for all fuels. Summaries of the engine and test operating conditions during the toluene and n-heptane mixtures tests and also the 1-octene and n-octane mixture tests are given in Tables 4 and 5.

2.4. Droplet sizing

Spray particle sizing for selected toluene/n-heptane mixtures was undertaken in a novel optical pressure chamber, the design

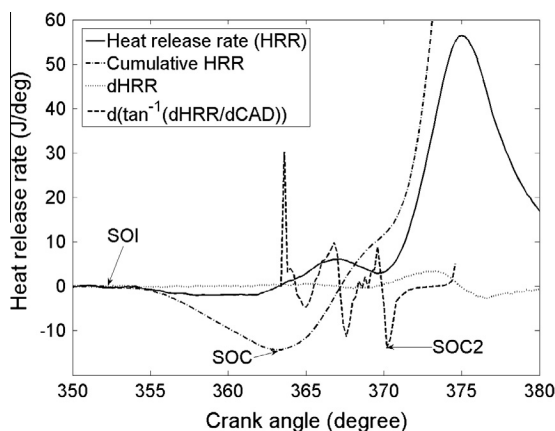


Fig. 2. Definition of SOC and SOC2 in terms of apparent net heat release rate (HRR), cumulative heat release rate, 1st derivative of heat release rate (dHRR) and $d(\tan^{-1}(dHRR/dCAD))$ where dCAD is the 1st derivative of the crank angle position.

of which has been described by Patel et al. [28]. The Sauter mean diameter (SMD) of spray droplets from a single hole injector was determined with the method of laser diffraction using an optical droplet sizing system (Malvern Spraytec Particle Sizer).

For all droplet sizing measurements, the fuel was injected at a pressure of 110 bar and a temperature of 17 °C into the optical pressure chamber, which was maintained at a constant gas pressure of 1 bar and a temperature of 17 °C. The optical droplet sizing system was aligned to intersect the fuel spray 60 mm below the injector nozzle tip, and horizontally displaced 10 mm off the central y-axis.

3. Results

3.1. Toluene/n-heptane binary mixtures

Figure 3 shows the in-cylinder pressures and apparent net heat release rates of the toluene/n-heptane binary fuel mixtures and reference fossil diesel at both constant injection and constant ignition timing. Apparent from Fig. 3 is that under both timing conditions, for the reference fossil diesel and toluene/n-heptane blends of up to 40% toluene, the majority of heat release occurs during premixed combustion (defined as the combustion of fuel and air mixed to combustible stoichiometry during the ignition delay period), as indicated by the rapid rise and subsequent fall in heat release rates following SOC. Also visible in Fig. 3, at both timing conditions, is the presence of two stage ignition for all toluene/n-heptane blends containing 25% or more toluene. The interval between the two ignition stages increases with the level of toluene present, resulting in the bulk of heat release rate occurring later into the expansion stroke for those blends containing more than 40% toluene. A binary mixture containing 52% toluene was found to combust in a steady manner only at constant ignition timing (Fig. 3), at constant injection timing the same blend did not ignite during every cycle, with any combustion that did occur commencing very late into the expansion stroke.

A further series of experiments were conducted where the ignition delay of the toluene/n-heptane binary mixtures was isolated as a variable by the use of the ignition improving additive 2 EHN. In an iterative process, the correct dosage of 2 EHN was found so that several blends with varying toluene content all exhibited the same ignition delay (within 0.2 CAD, the resolution of the shaft encoder utilised in the recording of in-cylinder pressure). These engine experiments were then performed at a fixed SOI of 7.5 CAD BTDC and also an injection timing of 6.2–6.4 CAD BTDC so that SOC always occurred at TDC.

Figure 4 shows the in-cylinder pressures and apparent net heat release rates of three toluene/n-heptane blends at constant ignition delay timings of fixed SOI and SOC at TDC. Despite the use of 2 EHN to equalize the ignition delay time, it can be seen that due to the two stage ignition delay observed in Fig. 3, the peak heat release rate of the 40% toluene blend still occurs later into the expansion stroke (Fig. 4). This is also true to a lesser extent of the 30% toluene mixture (Fig. 4). As in Fig. 3, it can be seen that the majority of heat release for all mixtures occurs during premixed combustion (Fig. 4).

Figures 5a and b show the duration of ignition delay and 2nd ignition delay of the toluene/n-heptane binary mixtures at constant injection and constant ignition timing. Where present in Figs. 5a and b, and in the following figures, the extent of the error bars given are plus and minus one standard deviation from the mean value (which is the point displayed on the plots) taken from repeat experimental runs of the same test fuel. The values of ignition delay presented in Fig. 5a are defined as the interval between SOI and the first appearance of positive apparent heat release for

Table 4
Engine and test operating conditions of toluene and n-heptane mixtures, at 1200 rpm and 450 bar injection pressure.

% Toluene	2 EHN dosage (ppm)	IMEP (bar)	Constant injection timing (SOI at 7.5 CAD BTDC)								Constant ignition timing (SOC at TDC)							
			Ignition delay (CAD)		Injection duration (μ s)		Indicated thermal efficiency (%)		Equivalence ratio (ϕ)		Ignition delay (CAD)		Injection duration (μ s)		Indicated thermal efficiency (%)		Equivalence ratio (ϕ)	
			Mean	1 δ	Mean	1 δ	Mean	1 δ	Mean	1 δ	Mean	1 δ	Mean	1 δ	Mean	1 δ	Mean	1 δ
Reference diesel	0	4	7.5	0.1	613	10	43.16	0.49	0.397	0.002	7.5	0.1	614	7	43.05	0.40	0.396	0.002
0.0	0	4	7.1	–	655	–	42.67	–	0.422	–	7.4	–	657	0	42.90	–	0.422	–
5.0	0	4	7.3	–	644	–	42.95	–	0.420	–	7.5	–	646	0	43.08	–	0.420	–
10.1	0	4	7.5	–	658	–	42.75	–	0.416	–	7.5	–	658	0	42.65	–	0.415	–
25.0	0	4	8.1	–	650	–	42.84	–	0.405	–	8.1	–	648	0	42.96	–	0.405	–
35.0	0	4	8.7	–	642	–	43.28	–	0.397	–	8.8	–	630	0	43.22	–	0.396	–
35.1	0	4	8.9	–	628	–	44.09	–	0.400	–	8.9	–	631	0	43.67	–	0.399	–
40.0	0	4	9.3	–	638	–	43.21	–	0.393	–	9.0	–	638	0	43.19	–	0.393	–
46.3	0	4	9.9	–	658	–	41.93	–	0.388	–	9.6	–	632	0	43.62	–	0.389	–
50.0	0	4	10.7	–	717	–	39.31	–	0.382	–	9.9	–	664	0	42.38	–	0.384	–
52.2	0	4	DNC	–	–	–	–	–	–	–	10.5	–	681	0	39.97	–	0.379	–
0.0	616	4	6.3	0.0	635	6	43.85	0.08	0.424	0.001	6.4	0.0	637	5	43.80	0.06	0.425	0.001
10.0	2063	4	6.3	–	622	–	43.74	–	0.419	–	6.2	–	618	0	43.91	–	0.419	–
19.8	5514	4	6.1	–	622	–	43.67	–	0.408	–	6.2	–	620	0	43.68	–	0.407	–
30.9	7876	4	6.1	–	620	–	43.77	–	0.404	–	6.2	–	617	0	43.78	–	0.404	–
40.0	10,780	4	6.3	–	639	–	43.65	–	0.393	–	6.4	–	638	0	43.58	–	0.393	–

Table 5
Engine and test operating conditions of 1-octene and n-octane mixtures, at 1200 rpm and 450 bar injection pressure.

% 1-Octene	2 EHN dosage (ppm)	IMEP (bar)	Constant injection timing (SOI at 7.5 CAD BTDC)								Constant ignition timing (SOC at TDC)							
			Ignition delay (CAD)		Injection duration (μ s)		Indicated thermal efficiency (%)		Equivalence ratio (ϕ)		Ignition delay (CAD)		Injection duration (μ s)		Indicated thermal efficiency (%)		Equivalence ratio (ϕ)	
			Mean	1 δ	Mean	1 δ	Mean	1 δ	Mean	1 δ	Mean	1 δ	Mean	1 δ	Mean	1 δ	Mean	1 δ
Reference diesel	0	4	7.1	0.1	617	2	42.70	0.24	0.397	0.000	7.2	0.0	619	3	42.40	0.16	0.397	0.000
0.0	0	4	6.5	–	615	–	42.12	–	0.422	–	6.5	–	618	–	42.01	–	0.421	–
10.0	0	4	6.5	–	616	–	42.27	–	0.420	–	6.7	–	621	–	42.30	–	0.420	–
25.0	0	4	6.9	–	617	–	42.30	–	0.418	–	6.8	–	619	–	42.05	–	0.418	–
50.0	0	4	7.3	–	619	–	41.84	–	0.415	–	7.4	–	621	–	42.14	–	0.415	–
63.1	0	4	7.3	–	617	–	42.09	–	0.412	–	7.4	–	620	–	42.00	–	0.411	–
75.0	0	4	7.5	–	615	–	42.15	–	0.410	–	7.7	–	620	–	42.28	–	0.410	–
87.5	0	4	7.7	–	618	–	42.59	–	0.408	–	7.8	–	621	–	42.13	–	0.408	–
95.0	0	4	7.9	–	617	–	42.31	–	0.407	–	8.0	–	623	–	42.41	–	0.407	–
100.0	0	4	8.1	–	617	–	42.24	–	0.406	–	8.1	–	618	–	42.08	–	0.406	–
0.0	441	4	5.9	–	619	–	41.90	–	0.422	–	5.9	–	619	–	42.12	–	0.421	–
50.0	8589.5	4	5.7	0.0	619	1	41.89	0.04	0.414	0.000	5.8	–	620	–	41.95	–	0.414	0.000
100.0	12,169	4	6.1	0.0	620	0	41.79	0.09	0.407	0.000	6.0	0.1	620	0	41.87	0.03	0.406	0.000

each fuel (SOC). The values of 2nd ignition delay presented in Fig. 5b are defined as the interval between initial fuel ignition (SOC) and the point at which a second phase of heat release commences (SOC2 as defined in Section 2.3).

Figure 5a shows that increasing the percentage of toluene present in the toluene/n-heptane binary mixtures from 0% to 30% results in an almost linear increase in the ignition delay time at both timing conditions. Beyond 35% toluene, while the effect on ignition delay of further increasing the level of toluene present remains linear, the gradient of this relationship increases significantly (Fig. 5a). An increase in the level of toluene from 10% to 20% results in an increase in ignition delay of approximately 0.5 CAD, whereas a similar 10% increase in the level of toluene from 40% to 50% results in a 2 CAD increase in ignition delay (Fig. 5a). Furthermore, the binary mixtures would no longer combust in a steady manner without misfiring at toluene levels beyond 50% and 52% at constant injection and constant ignition timing respectively. The ignition retarding effect of toluene is in agreement with

previous experimental results of toluene/n-heptane binary mixtures from shock tubes [9,11], rapid compression machines [4,17,18] and HCCI [12] and CFR [19] engines.

In Fig. 5b, it can be seen that at both injection timings the duration of 2nd ignition delay was less than 1 CAD for those toluene/n-heptane mixtures containing less than 25% toluene. At 35% toluene the duration of 2nd ignition delay has increased significantly to approximately 4 CAD, and at 50% toluene it rose to approximately 7 CAD (Fig. 5b). The potential mechanisms by which the presence of toluene affects the mixture reactivity, and thus the duration of both stages of ignition delay, are discussed in some detail in Section 4.1.

Figures 6a and b show the peak apparent net heat release rates, and coefficient of variation (COV) thereof, of the toluene/n-heptane and reference fossil diesel at constant injection, constant ignition and the constant ignition delay timings of fixed SOI and SOC at TDC. At constant injection and constant ignition timings, increasing the level of toluene present in the mixture from 0% to 10% results

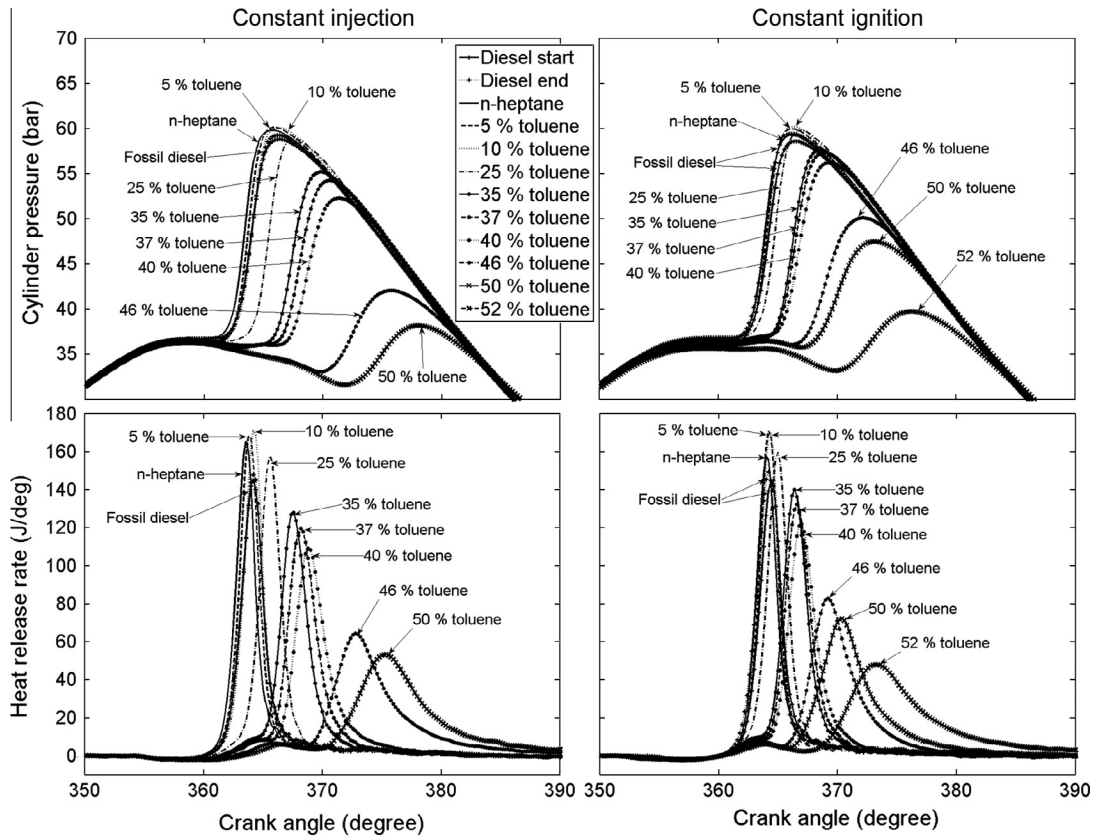


Fig. 3. In-cylinder pressures and apparent net heat release rates of toluene/n-heptane mixtures and reference fossil diesel at constant injection and constant ignition timing.

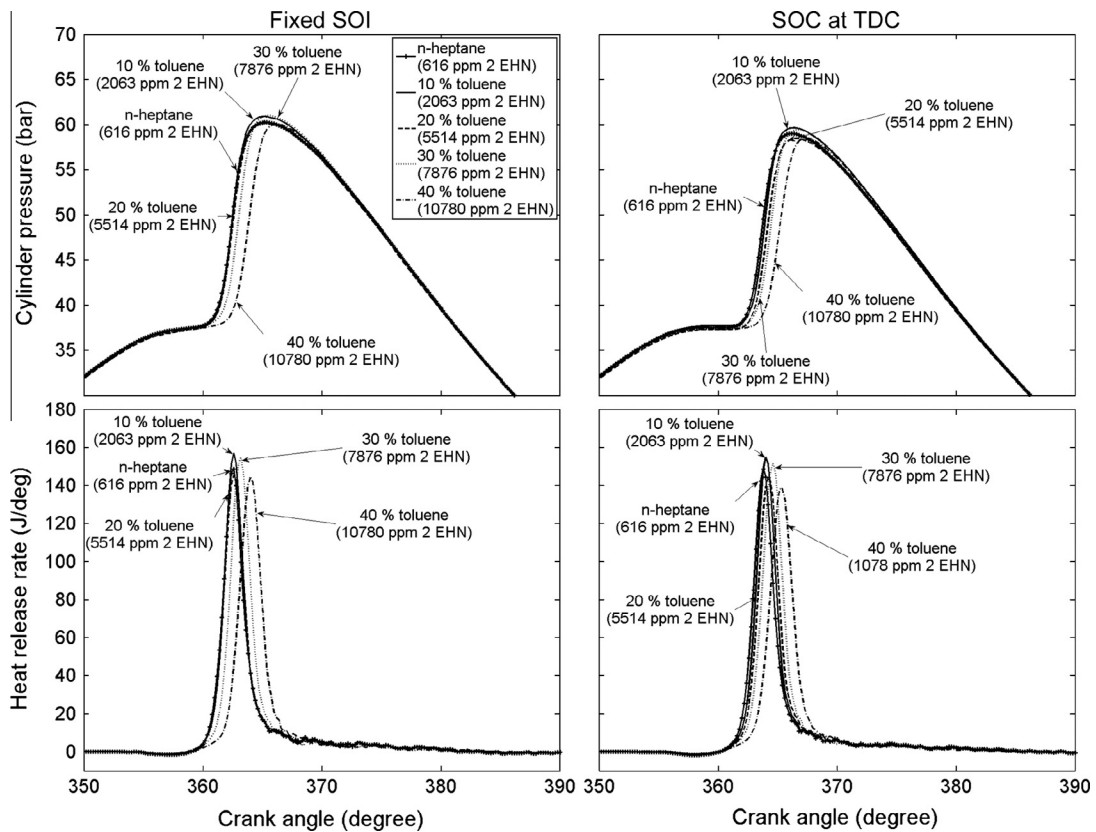


Fig. 4. In-cylinder pressures and apparent net heat release rates of toluene/n-heptane mixtures and reference fossil diesel at constant ignition delay fixed SOI and SOC at TDC timing.

in a slight increase in the peak heat release rate of approximately 160–170 J/deg (Fig. 6a). Further raising the percentage of toluene in the blend sees an increasing reduction in the peak heat release rate down to approximately 50 J/deg. The initial increase in peak heat release rate (between 0% and 10% toluene) can be explained by the concurrent increase in ignition delay (Fig. 6a). It has previously been observed [26] that an increased ignition delay time allows more time for fuel and air mixing prior to ignition and that this larger premixed burn fraction results in a higher peak heat release rate.

For those mixtures containing more than 25% toluene, the breakdown in this relationship (Figs. 5a and 6a), can be attributed to a visibly later time of peak heat release which is especially apparent at constant injection timing (Fig. 3). Furthermore, for mixtures containing 35% toluene and above (Fig. 3), it can be seen that this is due to the presence of two stage ignition (Fig. 5b). Concurrently, blends containing greater than 40% toluene show a significant increase in the COV of peak heat release rate (Fig. 6b). It follows that with heat release occurring further into the expansion stroke, more of the cylinder wall is exposed and so more heat transfer from the cylinder charge would occur, thus lowering the apparent peak heat release rate and also increasing cycle to cycle variability. Figure 6a shows that with the effect of ignition delay isolated, at both constant injection delay (CID) fixed SOI and SOC at TDC timing, no change in peak heat release rate with increasing levels of toluene is visible beyond the range of experimental error. However, when considering the heat release traces presented in Fig. 4, the mixture containing 40% toluene does appear to be subject to a longer 2nd ignition delay and lower peak heat release rate.

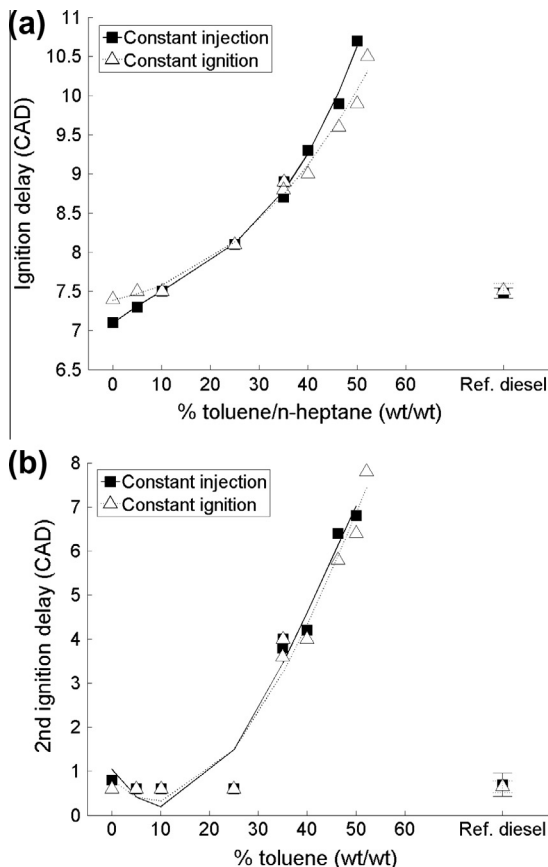


Fig. 5. Duration of ignition delay (a) and 2nd ignition delay (b) of toluene/n-heptane mixtures and reference fossil diesel at constant injection and constant ignition timing.

Figures 7a and b show the calculated maximum in-cylinder global temperature (assuming mixture homogeneity and ideal gas behavior) and time of occurrence of the toluene/n-heptane mixtures and reference fossil diesel at constant injection, constant ignition and CID timings of fixed SOI and SOC at TDC. At all injection timings, with and without ignition delay isolated, for blends containing up to 40% toluene the calculated maximum in-cylinder temperature and the time at which it occurs are relatively constant showing no apparent effect of the increasing level of toluene present (Figs. 7a and b). As the level of toluene exceeds 40%, maximum in-cylinder temperatures fall rapidly (Fig. 7a) and the temperatures are reached much further into the expansion stroke (Fig. 7b). A positive correlation with peak heat release rate could be expected (as a more intense release of energy will result in higher temperatures and has been previously observed [26]) and is apparent to a certain degree, with the lowest peak heat release rates resulting in the lowest maximum in-cylinder temperatures (Figs. 6a and 7a).

Figure 8 shows the exhaust gas NO_x emissions of the toluene/n-heptane mixtures and reference fossil diesel at constant injection, constant ignition and both CID timings. At constant injection and constant ignition timing, levels of NO_x emitted increase with the level of toluene present up to 40% (Fig. 8). Beyond 40% toluene present in the blend, NO_x emissions reduce drastically, mirroring both the decrease and later occurrence of the maximum in-cylinder temperature (Figs. 7a and b). This could be anticipated as the production of NO_x in compression ignition combustion is known to be highly thermally sensitive [29], both to the magnitude of the in-cylinder temperature and the residence time of the cylinder contents at elevated temperatures [30–32]. However, where NO_x

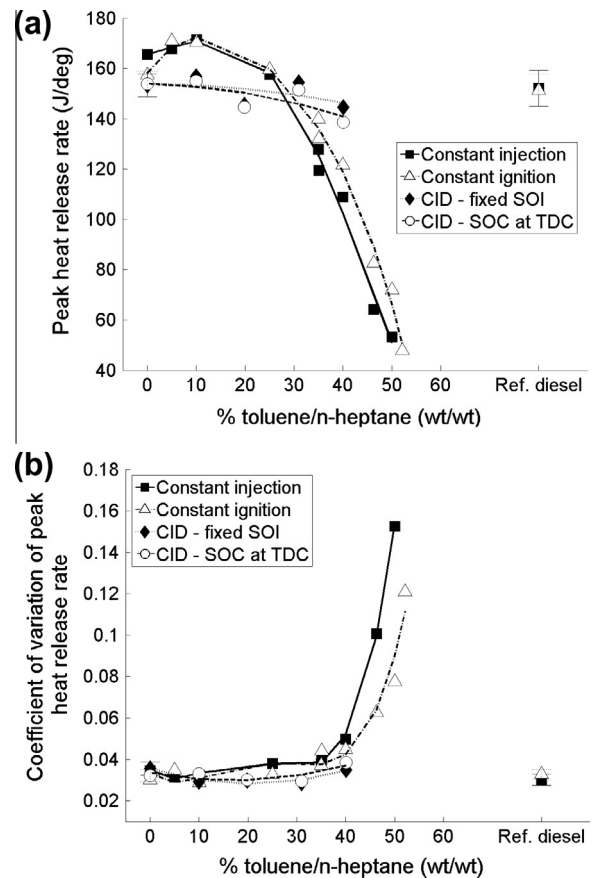


Fig. 6. (a) Peak apparent net heat release rates and (b) coefficient of variation of peak heat release rates of toluene/n-heptane mixtures and reference fossil diesel at constant injection, constant ignition and constant ignition delay timings.

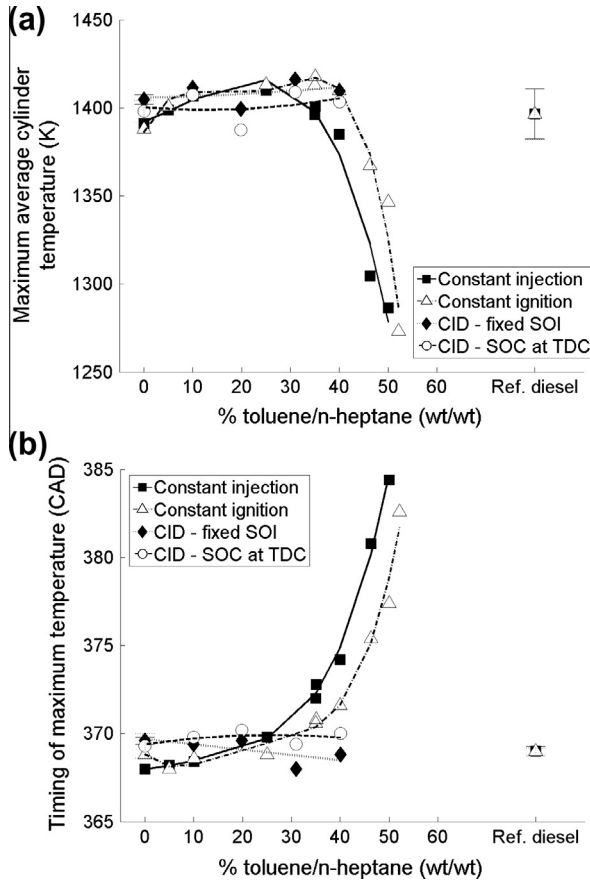


Fig. 7. (a) Calculated maximum in-cylinder global temperature and (b) time of occurrence of toluene/n-heptane mixtures and reference fossil diesel at constant injection, constant ignition and constant ignition delay timings.

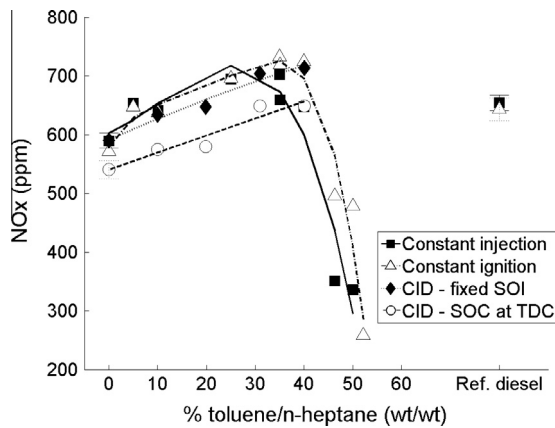


Fig. 8. Exhaust gas NOx emissions of toluene/n-heptane mixtures and reference fossil diesel at constant injection, constant ignition and constant ignition delay timings.

levels are increasing between 0% and 40% toluene (Fig. 8), there is no concurrent increase in the maximum in-cylinder temperature (Fig. 7a), nor does it occur earlier and increase the residence time of gases at conditions suitable for NOx production (Fig. 7b). Furthermore, with ignition delay isolated at CID timings, a similar increase in NOx emissions with between 0% and 40% toluene present in the mixtures occurs (Fig. 8), again with no indication that in-cylinder thermal conditions have become more conducive to NOx production (Figs. 7a and b). However, it must be noted that concur-

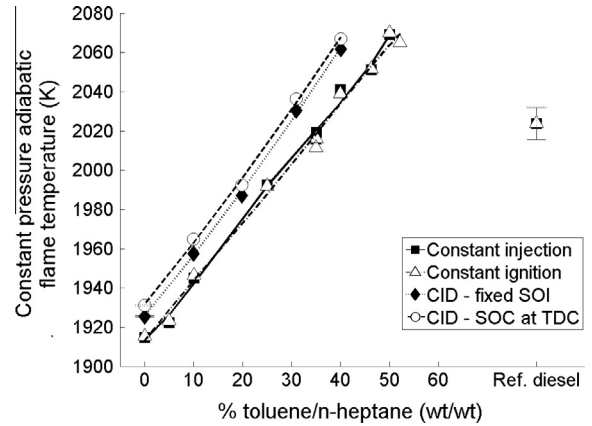


Fig. 9. Constant pressure adiabatic flame temperatures of toluene/n-heptane mixtures and reference fossil diesel at constant injection, constant ignition and constant ignition delay timings.

rent to increasing NOx emissions, is the increasing addition of 2 EHN to maintain constant ignition delay, the presence of which is known to contribute disproportionately to NOx emissions. The increase in NOx emissions at constant injection and constant ignition timing, up to a toluene content of 40%, is in agreement with the CFR engine study of Xiao et al. [19], while the similar increase at constant ignition delay timings is not.

Figure 9 shows the constant pressure adiabatic flame temperatures of the toluene/n-heptane mixture and reference fossil diesel at constant injection, constant ignition and both CID timings. The adiabatic flame temperature at constant pressure was calculated, assuming an equivalence ratio of 1 using the method described by Turns [33], and taking into account dissociation of CO₂, H₂O and N₂. The initial temperature of the reactants was taken as the calculated minimum in-cylinder global temperature between SOI and SOC. The calculations were performed for the binary mixtures using literature values of the enthalpy of formation of toluene and n-heptane in a gaseous state [34,35]. It can be seen in Fig. 9, that as the percentage of highly unsaturated toluene increases in the blend, the constant pressure adiabatic flame temperature does so as well. Therefore, notwithstanding the possible influence of 2 EHN content, it is suggested that the increasing adiabatic flame temperature (Fig. 9) is the primary driver of the increase in NOx emissions at all timing conditions for mixtures containing 0–40% toluene (Fig. 8). The adiabatic flame temperature continues to increase with mixtures containing more than 40% toluene (Fig. 9), however this is not sufficient to offset the changes in combustion phasing and in-cylinder thermal conditions that dramatically reduce the level of NOx produced (Fig. 8).

Figures 10a and b show the exhaust gas emissions of CO and THC of the toluene/n-heptane mixtures and reference fossil diesel at constant injection, constant ignition and CID timings. At constant injection and constant ignition timing, both CO and THC emissions increase with the level of toluene present in the binary mixtures (Figs. 10a and b), and for the latter the increase becomes exponential at around 40% toluene (Fig. 10b), coinciding with the dramatic decrease in maximum in-cylinder temperatures (Fig. 7a). CO and THC are known to be products of incomplete combustion, and indicate the increasing existence of both fuel rich and fuel lean regions within the cylinder contents as the level of toluene in the fuel blend and the ignition delay time and 2nd ignition delay increases (Fig. 5a and b). Meanwhile, the increasing ignition delay time (Fig. 5a) allows for greater fuel over-dilution. At CID timings, with ignition delay equalised, emissions of CO and THC continue to show an increase with the percentage of toluene present in the mixture (Figs. 10a and b), albeit much less steeply. The

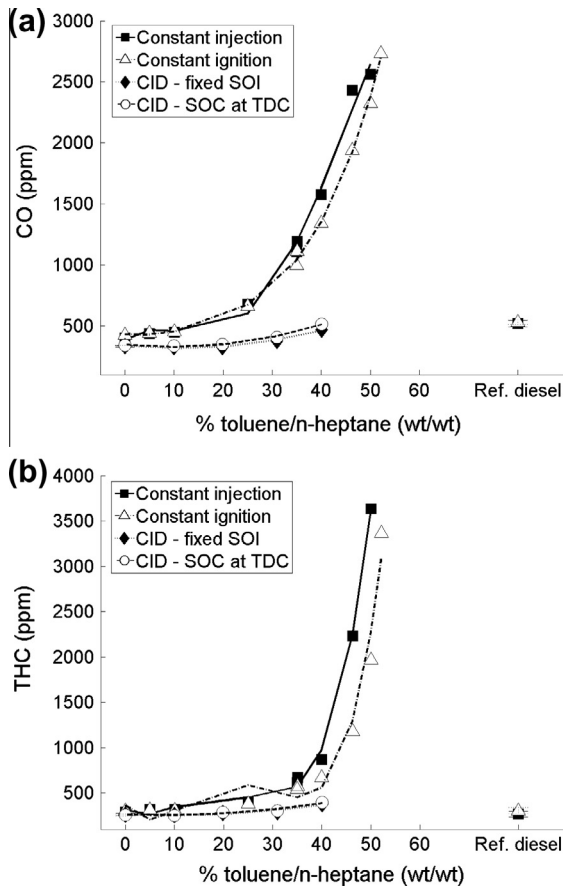


Fig. 10. CO (a) and THC (b) emissions of toluene/n-heptane mixtures and reference fossil diesel at constant injection, constant ignition and constant ignition delay timings.

peak heat release rates of the blends containing 30% and 40% toluene did occur slightly later than those of lesser toluene content (Fig. 4), and it can be seen that combustion phasing and in-cylinder conditions are the primary driver in determining the exhaust level emissions of CO and THC. However, a secondary influence of the properties of toluene relative to those of n-heptane may also be contributing to the trends of increasing CO and THC emissions with increasing toluene content visible in Figs. 10a and b. One such property may be the higher carbon to hydrogen ratio of toluene relative to n-heptane, which would increase the level of carbon oxidation occurring relative to that of hydrogen for a constant release of energy. It can also be seen that toluene has a higher density, viscosity and boiling point than n-heptane (Table 2), and so it is tentatively suggested that these factors produce increasingly poor fuel and air mixing as the level of toluene in the blend increases.

Figures 11a and b show the particle emissions of the toluene/n-heptane binary mixtures and reference fossil diesel at constant injection and constant ignition timings. At both constant injection and constant ignition timing (Figs. 11a and b), there is no clear influence of the percentage toluene apparent on the number of ultrafine ($D_p < 20$ nm) particles produced. However, at constant injection timing (Fig. 11a), it can be seen that increasing the level of toluene in the binary mixture decreases the number of nucleation mode particles ($20 \text{ nm} < D_p < 50$ nm). This relationship between toluene content and particle number in this size range is not precisely monotonic, and is increasingly less apparent when considering larger accumulation mode particles ($D_p > 50$ nm). Indeed, it can be seen that the distribution of particle number with toluene content converges at a particle diameter of approximately

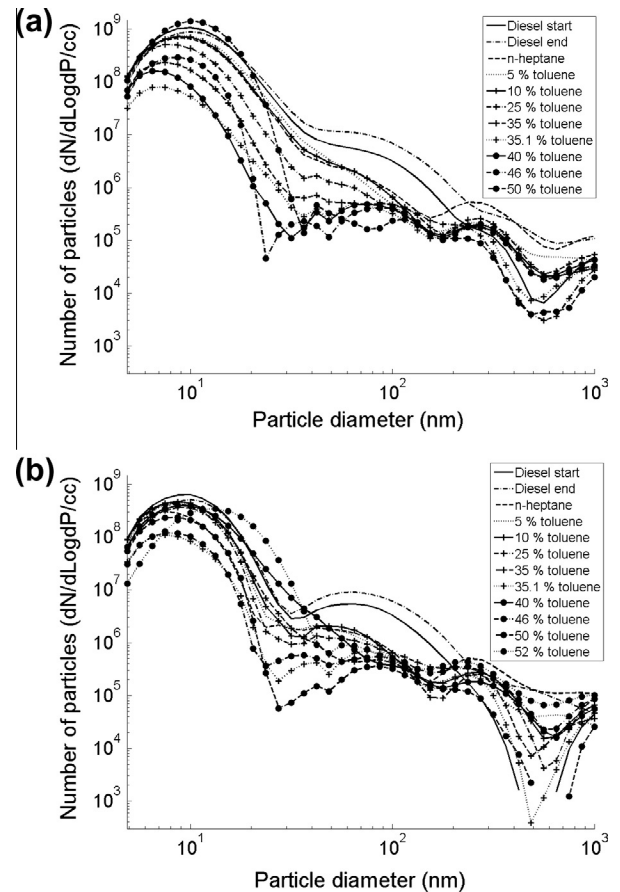


Fig. 11. Particle emissions of toluene/n-heptane mixtures and reference fossil diesel at (a) constant injection and (b) constant ignition timings.

100 nm, and the subsequent distribution at larger particle sizes is entirely non-monotonic (Fig. 11a). At constant ignition timing (Fig. 11b), the distribution of particle number with percentage toluene is tighter than at constant injection timing (Fig. 11a) up to a particle diameter of 300 nm; this indicates a strong influence of combustion phasing (Fig. 3) on the production of particulates of all sizes. Therefore, it is suggested that the effect of increased toluene content reducing the number of nucleation mode particles ($D_p < 50$ nm) observed at constant injection timing (Fig. 11a) can most likely be attributed to the influence of toluene content on the binary mixture ignition delay. Nucleation mode particles initially form in fuel rich zones [36], and it can be seen that where increased toluene content increases the ignition delay time (Figs. 5a and b), and there is more time for fuel and air mixing prior to SOC, that the prevalence of these zones will decrease. Furthermore, there is a concurrent decrease in the fuel air equivalence ratio (Table 4) with increasing percentage toluene present.

Figures 12a and b show the particle emissions of the toluene/n-heptane binary mixtures at fixed SOI and SOC at TDC constant ignition delay timing conditions. At both constant ignition delay timings, a near monotonic relationship of increasing toluene content reducing the number of nucleation mode particles ($20 \text{ nm} < D_p < 50$ nm) is apparent (Figs. 12a and b). As with the same observation made at constant injection and constant ignition timing (Figs. 11a and b), no such relationship is visible for accumulation mode particles of diameter greater than 70 nm. Toluene is known to have a higher sooting tendency than n-heptane in both premixed and laminar diffusion flames [37,38] and has previously been observed to increase smoke emissions in binary mixtures of

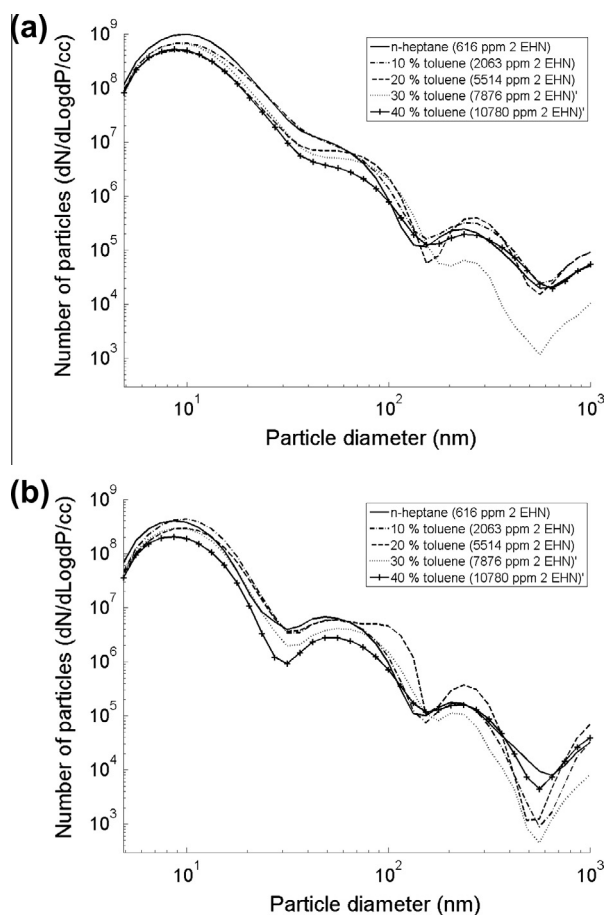


Fig. 12. Particle emissions of toluene/n-heptane mixtures and reference fossil diesel at constant ignition delay timings, (a) fixed SOI and (b) SOC at TDC.

n-heptane and up to 20% (wt/wt) toluene [19]. However, no previous observations of the effect of toluene presence on the production nucleation mode particles ($D_p < 50$ nm) have been widely reported. It is therefore suggested that the observed decrease in the number of nucleation mode particles produced with increasing toluene content, regardless of combustion phasing, can be primarily attributed to decreasing equivalence ratio (Table 4). A second and more speculative hypothesis is that the reduced number of nucleation mode particles can be explained by the nuclei from

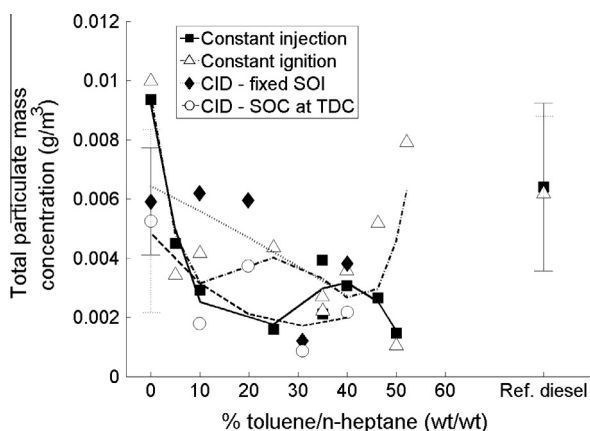


Fig. 13. Exhaust gas total particulate mass emissions of toluene/n-heptane mixtures and reference fossil diesel at constant injection, constant ignition and constant ignition delay timings.

toluene forming more easily and earlier than those from n-heptane. Thus less nucleation mode particles are apparent in the exhaust gas where the toluene content has increased, as a greater percentage of the nuclei formed experienced sufficient time for surface growth and agglomeration.

Figure 13 shows the total particulate mass emitted by the toluene/n-heptane mixtures and reference fossil diesel at constant injection, constant ignition and both constant ignition delay timings. Notwithstanding the range of error present in Fig. 13, the absence of any clear effect of toluene content on the mass of particulates produced is contrary to earlier observations [19,37,38]. This would suggest that any such influence of toluene is secondary to the combustion phasing and test to test variability at these test conditions. Furthermore, it would indicate that the observed decrease in nucleation mode particles with increasing toluene content (Figs. 11a and b, 12a and b) cannot be attributed to a greater tendency of nuclei from toluene to form larger particles.

3.2. 1-Octene/n-octane binary mixtures

Figure 14 shows the in-cylinder pressures and apparent net heat release rates of the 1-octene/n-octane binary mixtures at constant injection and constant ignition timings. It can be seen that regardless of the level of 1-octene present in the blend, the vast majority of heat release occurs during premixed combustion, and that none of the mixtures exhibit appreciable two-stage ignition (Fig. 14). This is in contrast to the binary mixtures of toluene/n-heptane (Fig. 3), but is to be expected when considering the closer values of cetane numbers for the components of the 1-octene/n-octane mixtures compared to those for the toluene/n-heptane mixtures (Table 2).

Employing the same methodology as applied in the case of the toluene/n-heptane binary mixtures (Section 3.1), a further series of experiments were conducted where the ignition delay of the 1-octene/n-octane binary mixtures was isolated as a variable by the use of the ignition improving additive 2 EHN. As such, Fig. 15 shows the in-cylinder pressure and apparent net heat release rates of the 1-octene/n-octane binary mixtures at the constant ignition delay timings of fixed SOI and SOC at TDC. With the initial ignition delay periods equalised, a 2nd ignition delay stage is suggested by the later time of peak heat release as the level of 1-octene present in the blend increases, resulting in a later occurrence of peak heat release rate (Fig. 15). A similar observation was made of the toluene/n-heptane mixtures in which 2 EHN had been used to equalise the duration of the initial ignition delay period (Fig. 4), and suggests that the pool of ignition advancing radicals provided by the 2 EHN are consumed during the 1st ignition delay period and are no longer available during the 2nd ignition delay period.

Figures 16a and b show the duration of ignition delay and 2nd ignition delay of the 1-octene/n-octane binary mixtures and reference fossil diesel at constant injection and constant ignition timing. Increasing the percentage of 1-octene present in blends results in an approximately linear increase in ignition delay at both timing conditions (Fig. 16a), though between 80% and 100% 1-octene the gradient of increase does appear to be slightly steeper. This is possibly suggestive of a disproportionate ignition enhancing influence of small quantities of n-octane where the majority of the mixture is 1-octene. No variation in the duration of the 2nd ignition delay outside the resolution of the shaft encoder (0.2 CAD) is visible in measurements of in-cylinder pressure (Fig. 16b). Discussion as to the influence of 1-octene on the reactivity of 1-octene/n-octane mixtures is made in Section 4.2, and contrasted with the potential interactions between toluene and n-heptane discussed in Section 4.1.

Figure 17 shows the peak apparent net heat release rates of the 1-octene/n-octane binary mixtures and reference fossil diesel at

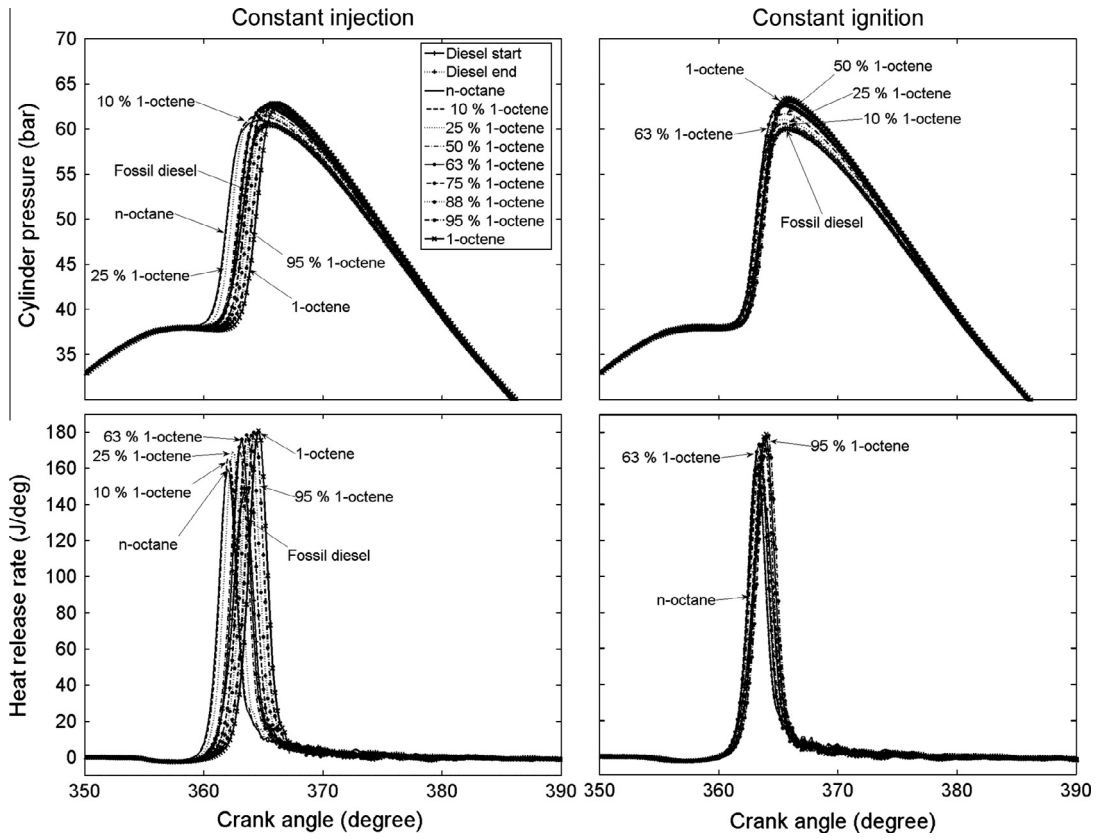


Fig. 14. In-cylinder pressures and apparent net heat release rates of 1-octene/n-octane mixtures and reference fossil diesel at constant injection and constant ignition timing.

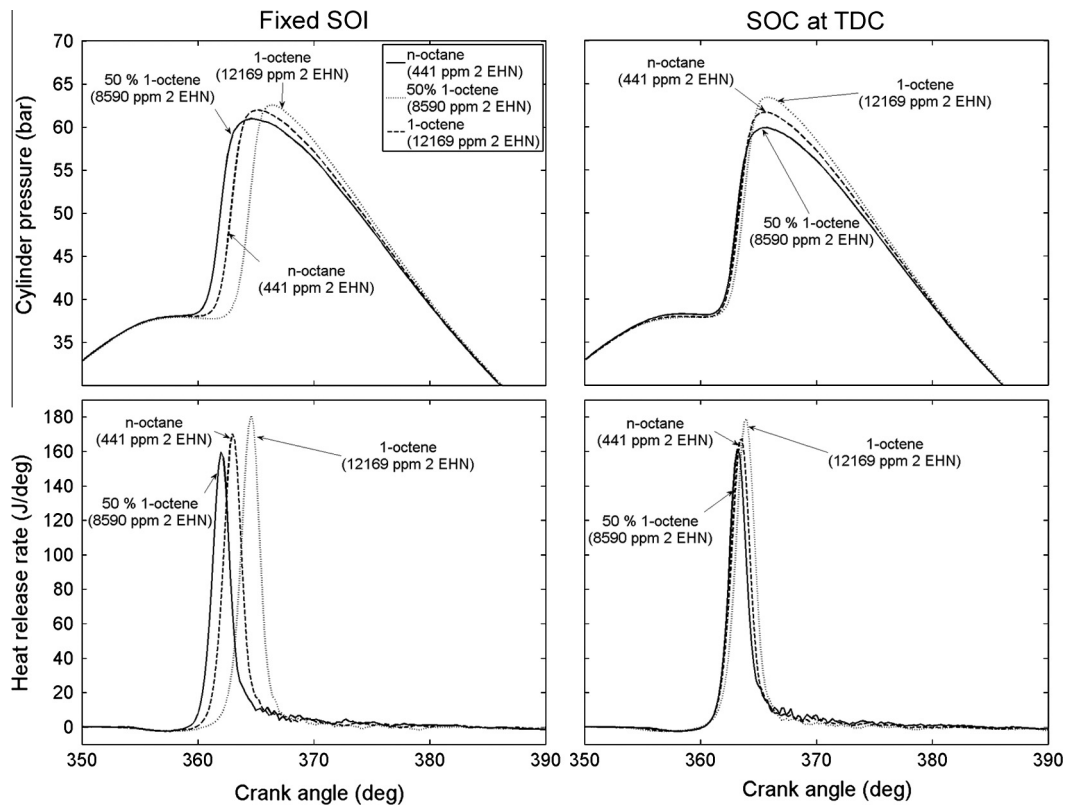


Fig. 15. In-cylinder pressures and apparent net heat release rates of 1-octene/n-octane mixtures and reference fossil diesel at constant ignition delay fixed SOI and SOC at TDC timing.

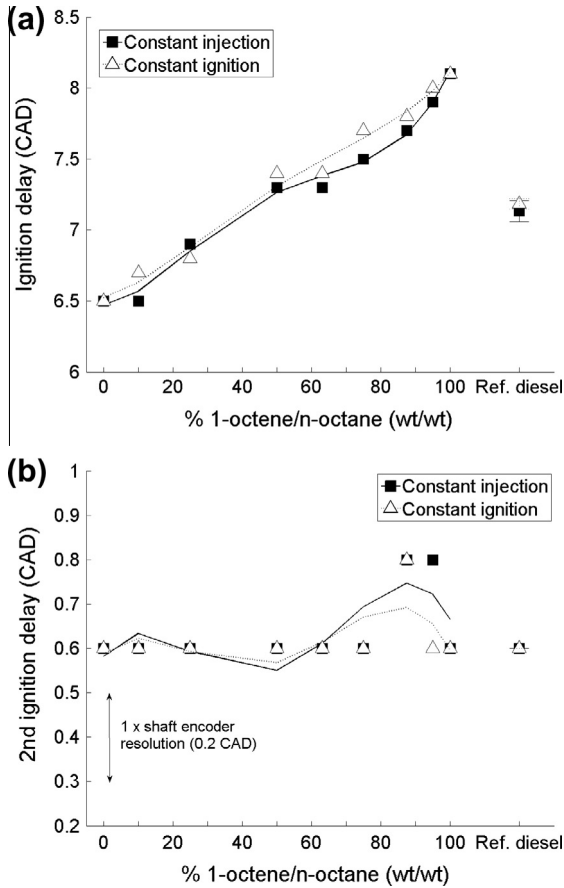


Fig. 16. (a) Duration of ignition delay and (b) 2nd ignition delay of 1-octene/n-octane mixtures and reference fossil diesel at constant injection and constant ignition timing.

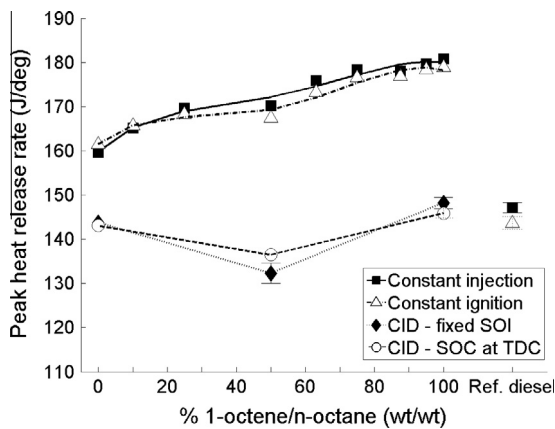


Fig. 17. Peak apparent net heat release rates of 1-octene/n-octane mixtures and reference fossil diesel at constant injection, constant ignition and constant ignition delay timings.

constant injection, constant ignition and the constant ignition delay timings of fixed SOI and SOC at TDC. At both constant injection and constant ignition timings there is a clear linear trend of increasing peak heat release rates with the level of 1-octene present in the blends (Fig. 16). This is consistent with the observed trend in ignition delay (Fig. 16a), and the relatively small range in ignition delay (6.5–8.1 CAD) means there is no breakdown in

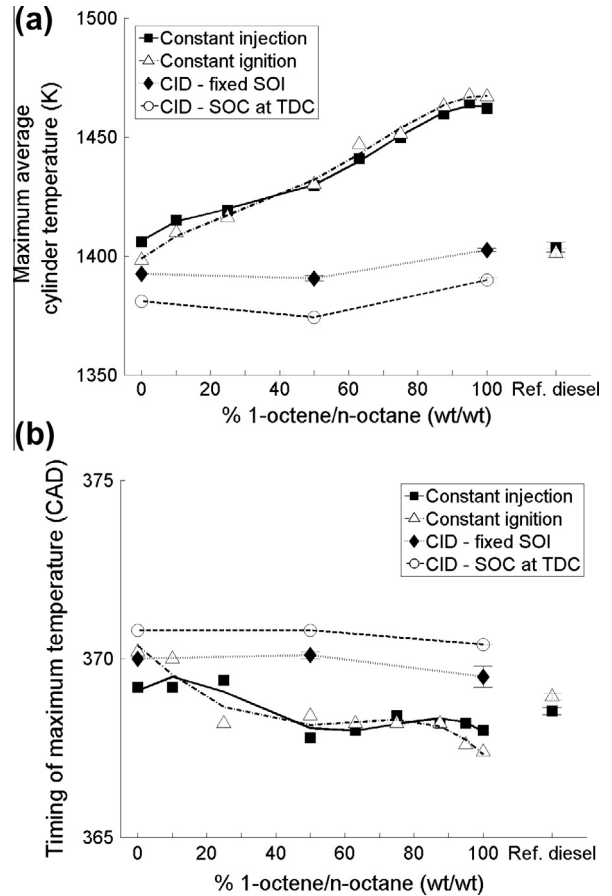


Fig. 18. (a) Calculated maximum in-cylinder global temperature and (b) time of occurrence of maximum in-cylinder temperature for 1-octene/n-octane mixtures and reference fossil diesel at constant injection, constant ignition and constant ignition delay timings.

the relationship between ignition delay and peak heat release rate as seen in the case of the toluene/n-heptane mixtures (Figs. 5a and 6a) as the majority of heat release for all blends occurs near TDC. For this reason there is also no significant difference between tests conducted at constant injection timing and those at constant ignition timing (Fig. 17). With the effect of ignition delay removed (Fig. 17), at both fixed SOI and SOC at TDC, the mixture containing 50% 1-octene displayed lower peak heat release rate than either n-octane or 1-octene (Fig. 17). However, this trend is in agreement with that which could be expected when considering that the method of equalizing ignition delay was not able to do so at an accuracy greater than \pm the shaft encoder resolution of 0.2 CAD (Table 5).

Figures 18a and b show the calculated maximum in-cylinder global temperature and time of occurrence of the 1-octene/n-octane binary mixtures and reference fossil diesel at constant injection, constant ignition and both constant ignition delay timings. Increasing the level of 1-octene present in the binary mixtures results in a higher maximum in-cylinder temperature (Fig. 18a) which also occurs earlier into the expansion stroke (Fig. 18b). This correlates well with the peak heat release rates of the binary mixtures (Fig. 17), those mixtures which displayed the highest peak heat release rate reach higher maximum in-cylinder temperatures more quickly than those mixtures which displayed lower peak heat release rates (Figs. 18a and b). It follows that a more concentrated release of energy, owing to longer ignition delay and greater premixed combustion, will result in higher and earlier temperatures when combustion is occurring near TDC where

changes in cylinder volume are minimal. At constant ignition delay timings (Fig. 18b), the maximum in-cylinder temperature again mirrors the peak heat release rate (Fig. 17) and so the slightly higher in-cylinder temperature reached by 1-octene can likely be attributed to the small residual differences in ignition delay (Table 5). There is, however, a notable offset between tests conducted at fixed SOI and those at SOC at TDC timing, with the latter condition consistently producing higher temperatures (Fig. 18a) despite similar levels of peak heat release rate (Fig. 16). There is also a consistent offset between the two timing conditions when considering the timing of maximum in-cylinder temperature (Fig. 18b) and the earlier occurrence of the maximum in-cylinder temperature at SOC at TDC timing explains the higher temperatures reached.

Shown in Fig. 19 are the exhaust gas NO_x emissions of the 1-octene/n-octane binary mixtures and reference fossil diesel at constant injection, constant ignition and the constant ignition delay timings of fixed SOI and SOC at TDC. At constant injection and constant ignition timing, with an increasing percentage of 1-octene present in the blends, levels of NO_x also increase linearly (Fig. 19). Clearly apparent is a strong correlation between the level of NO_x emitted and the in-cylinder thermal conditions, the highest levels of NO_x were emitted by pure 1-octene which also displayed the highest maximum in-cylinder temperature (Fig. 18a). At constant ignition delay timings, there is also a linear increase in NO_x emissions with increasing 1-octene content (Fig. 19), despite the mixture containing 50% 1-octene displaying a lower maximum in-cylinder temperature (Fig. 18a) occurring at approximately the same time (Fig. 18b) as that consisting of just n-octane. While the increasing presence of 2 EHN must again be noted, this suggests an effect of 1-octene on the level of NO_x emitted outside that of affecting the ignition delay time and subsequently the peak heat release rate and thereby maximum in-cylinder temperature reached. Furthermore, close inspection of Fig. 18a shows that at constant injection and constant ignition timings, between 90% and 100% 1-octene there is no increase in maximum in-cylinder temperature but NO_x levels continue to increase (Fig. 19). This could plausibly be due to the timing of maximum in-cylinder temperature (Fig. 18b), which does advance with the increase of 90–100% 1-octene in the mixtures resulting in a higher residence time for gases at elevated temperatures suitable for NO_x production. However, none of the non-linearity apparent in the time of maximum in-cylinder temperature (Fig. 18b) is apparent in the levels of NO_x emitted (Fig. 19).

Figure 20 shows the constant pressure adiabatic flame temperatures of the 1-octene/n-octane binary mixtures and reference fos-

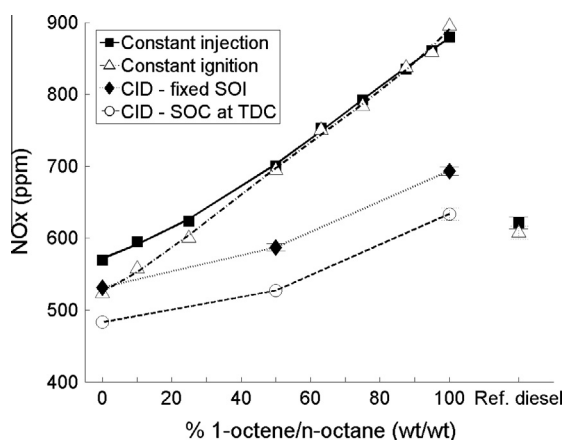


Fig. 19. Exhaust gas NO_x emissions of 1-octene/n-octane mixtures and reference fossil diesel at constant injection, constant ignition and constant ignition delay timings.

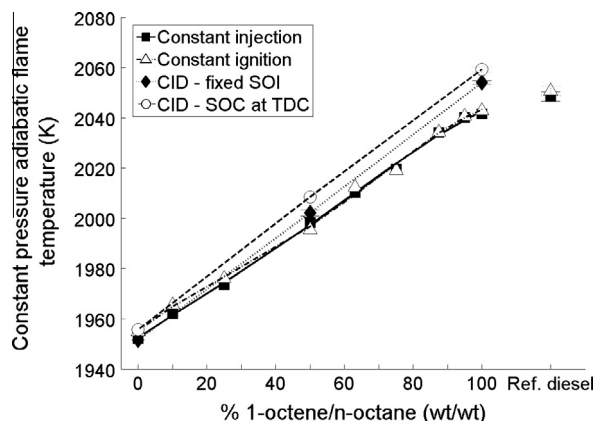


Fig. 20. Constant pressure adiabatic flame temperatures of 1-octene/n-octane mixtures and reference fossil diesel at constant injection, constant ignition and constant ignition delay timings.

sil diesel at all timing conditions. The constant pressure adiabatic flame temperatures of the 1-octene/n-octane blends were calculated according to the same method as employed in the calculation of the adiabatic flame temperatures of the toluene/n-heptane mixtures (Section 3.1), with values for the enthalpy of formation of 1-octene and n-octane obtained from literature [35,39]. It can be seen that there is a linear increase in the adiabatic flame temperature with the level of 1-octene present (Fig. 20), and so it is suggested that this is contributing to the trend of increasing NO_x emissions at all timing conditions (Fig. 19). This is in agreement with previous studies where the higher adiabatic flame temperature of 1-octene relative to n-octane has been identified as generating higher NO_x emissions where ignition delays have been equalised [24,26].

Figures 21a and b show the exhaust gas emissions of CO and THC of the 1-octene/n-octane binary mixtures and reference fossil diesel at constant injection, constant ignition and both constant ignition delay timings. At constant injection and constant ignition timing, increasing the level of 1-octene in the mixture results in an increase in CO levels (Fig. 21a) but has no clear influence on the emission of THC (Fig. 21b). At fixed SOI and SOC at TDC timing, where the ignition delay time has been equalized, there is no apparent influence of 1-octene levels on the emission of either CO or THC (Figs. 21a and b). This would imply that the increase in CO emissions observed at constant injection and constant ignition timing (Fig. 21a) is more likely attributable to the effect of 1-octene on combustion phasing than any physical property (Table 2).

Figures 22a and b show the particle emissions of the 1-octene/n-octane mixtures and reference fossil diesel at constant injection and constant ignition timings. At constant injection and constant ignition timings (Figs. 22a and b), no effect of increasing 1-octene content on the level of nucleation mode particles ($D_p < 50$ nm) can be seen. However, at constant ignition timing (Fig. 22b), there is a general decrease in accumulation mode particles ($50 \text{ nm} < D_p < 90$ nm) with increasing 1-octene content (though the relationship cannot be described as monotonic). A similar observation was made in the case of the toluene/n-heptane binary mixtures (Figs. 11a and b), albeit at a lower particle diameter, and was attributed to a change in the mixture stoichiometry with increasing toluene content. It can be seen that increasing 1-octene content in the binary mixtures of 1-octene/n-octane reduced the fuel air equivalence ratio (Table 5), and is concurrent with an increase in the ignition delay period (Fig. 16); both factors may potentially reduce the occurrence of fuel rich zones.

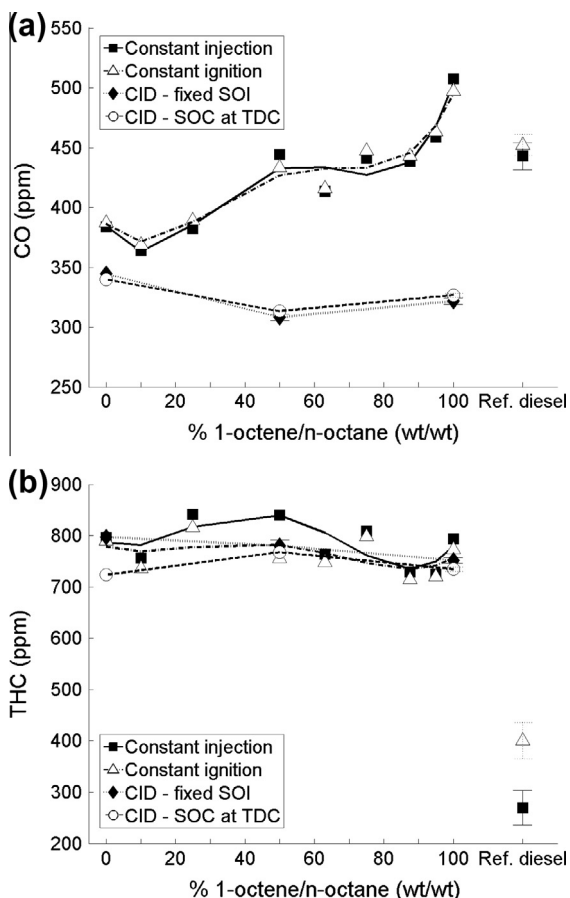


Fig. 21. CO (a) and THC (b) emissions of 1-octene/n-octane mixtures and reference fossil diesel at constant injection, constant ignition and constant ignition delay timings.

Shown in Figs. 23a and b are the particle emissions of the 1-octene/n-octane binary mixtures, at both constant ignition delay timings. At neither fixed SOI, or SOC at TDC timing, can a monotonic relationship between 1-octene percentage and particle number at any particle diameter be clearly discerned (Figs. 23a and b). This is contrary to the blends of toluene/n-heptane, where an observed relationship between toluene content and the number of nucleation mode particles persisted when ignition delay was eliminated as a variable (Figs. 11 and 12). Furthermore, it suggests that in the case of the 1-octene/n-octane binary mixtures, effects of combustion phasing dominate those of global stoichiometry or alkene chemistry.

Figure 24 shows the total mass of particulates emitted by the 1-octene/n-octane binary mixtures and reference fossil diesel at all timing conditions. At constant injection and constant ignition timing, the range of error presented does not make it possible to draw any conclusions as to the effect of 1-octene in the mixtures. Furthermore, no clear trends are readily apparent (Fig. 24), and no effect of the observed decrease in the number of accumulation mode particles with the increasing presence of 1-octene (Fig. 22b) can be discerned. However, at both constant ignition delay timings, the mixture containing 50% 1-octene produced significantly more particulate mass than either n-octane or 1-octene (Fig. 24). This is plausibly due to the thermal sensitivity of soot oxidation, (the rates of which increase with temperature [36]) as the 50% 1-octene mixture displayed a lower peak heat release rate than either pure n-octane or 1-octene (Fig. 17).

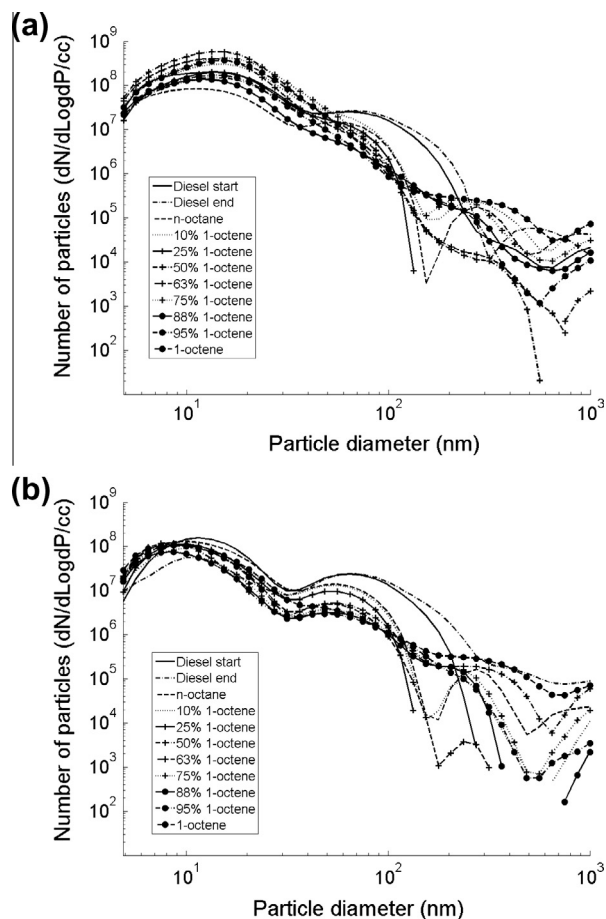


Fig. 22. Particle emissions of 1-octene/n-octane mixtures and reference fossil diesel at (a) constant injection and (b) constant ignition timings.

4. Discussion

4.1. Effect of toluene content on toluene/n-heptane binary mixture reactivity

The effect of increasing toluene content in a binary mixture with n-heptane is consistent with results of previous studies [9,11,12,17,18] in so much as that the mixture reactivity is decreased and the ignition delay time increased (Figs. 3, 5a and 5b). However, developing an understanding as to how toluene is impacting on the ignition process in the current study is not straightforward as the experimental conditions are somewhat different to the previous studies mentioned. Perhaps most significantly, the binary mixtures were directly injected at high pressures (450 bar) into the cylinder near TDC, with only limited time for fuel and air mixing prior to autoignition, creating a non-homogeneous cylinder charge. In the case of the studies conducted on high pressure shock tubes and rapid compression machines the fuel mixtures were evaporated and in some cases allowed to mix with the charge air for ten minutes prior to compression. Therefore, before considering the influence of toluene on the low temperature reaction chemistry of n-heptane, it is sensible to explore any possible effect of the physical properties of toluene on the efficiency of fuel and air mixing.

As suggested in Section 3.1, the higher density, viscosity and boiling point of toluene relative to n-heptane are likely to reduce the efficiency of fuel and air mixing (Table 2). Figure 25 shows the variation with injection pressure of the SMD of pure toluene, a toluene/n-heptane binary mixture of 50% toluene and n-heptane from a single hole injector measured with an optical droplet sizing

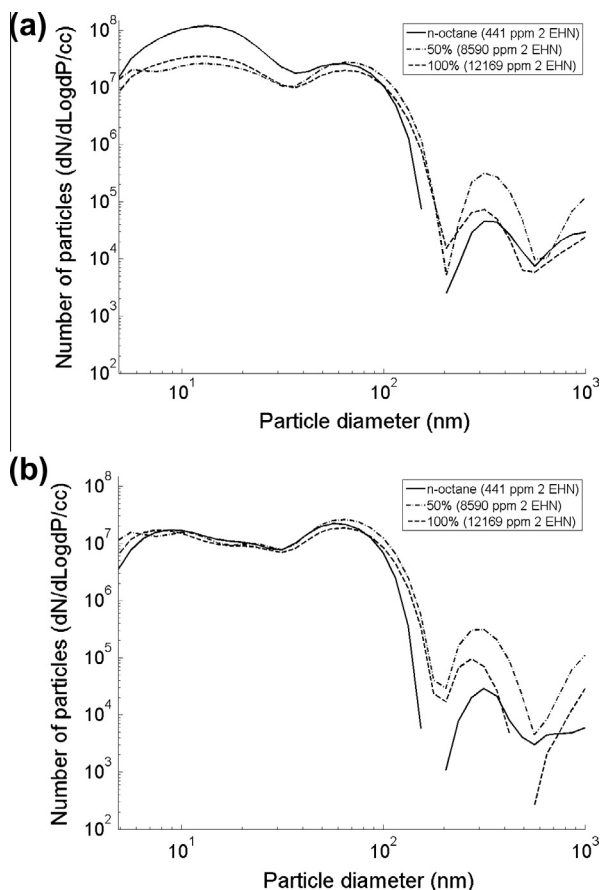


Fig. 23. Particle emissions of 1-octene/n-octane mixtures at constant ignition delay timings, (a) fixed SOI and (b) SOC at TDC.

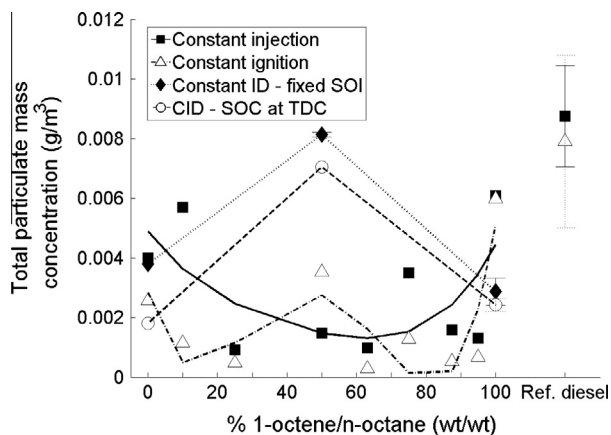


Fig. 24. Exhaust gas total particulate mass emissions of 1-octene/n-octane mixtures and reference fossil diesel at constant injection, constant ignition and constant ignition delay timings.

system (Section 2.4). While the measurements presented in Fig. 25 were conducted at much lower injection pressures than the engine experiments (110 vs. 450 bar), it can be seen that the droplet size of the 50% toluene mixture lies between that of pure toluene and n-heptane at all pressures. Therefore, it can be assumed that the physical properties of the binary mixtures corresponds proportionally to those of the components, thus increasing the percentage of toluene in the mixture would have reduced the efficiency of fuel and air mixing. If these changes in physical properties were significantly affecting the fuel and air mixing then an indication might

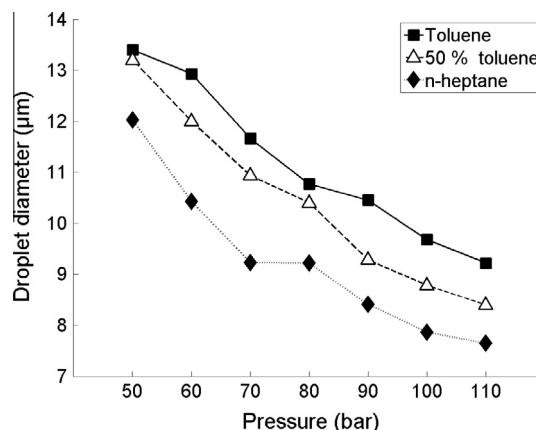
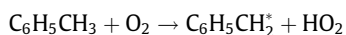


Fig. 25. Variation with injection pressure of mean spherical droplet diameter of toluene, 50% toluene binary mixture and n-heptane.

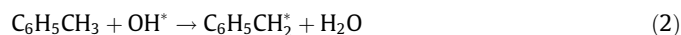
be provided by the toluene/n-heptane mixtures in which ignition delay was equalized (Fig. 4). Peak heat release rate has been previously observed to correspond well with the extent of the premixed fraction [26], and where the duration of ignition delays are equal, it follows that the premixed burn fraction will be dictated by the efficiency of fuel and air mixing prior to SOC. Therefore, with physical properties becoming less favorable for air and fuel mixing, with increasing percentage of toluene (equal ignition delay time), the observed peak heat release rate could be expected to decrease (Fig. 6a). While Fig. 6a does hint at such a trend, the extent of the error bars is relatively substantial and the lower peak heat release rate of the blend containing 40% toluene can be attributed to a later time of occurrence. Therefore, while an effect of changing physical properties is a potential influence on the mixture reactivity, the likely importance (if any) of such properties relative to other factors is minimal. Vanhove et al. [18] did suggest that the ignition inhibiting influence of toluene on n-heptane could not be attributed to chemical effects, however, the compression pressure of the RCM study on which this assertion is based was significantly lower than that for the current study (4 vs. 37 bar).

Toluene, as a single component and unlike n-heptane, has been observed to exhibit no low temperature reactivity that results in heat release [40]. However, Figs. 3 and 5b would seem to suggest that addition of toluene results in an increasingly significant 2nd ignition delay period that is not present at all in the case of pure n-heptane and binary mixtures containing less than 25% toluene. Previous studies have reported that addition of toluene diminishes the presence of the NTC and distinct two stage ignition [9,11]. However, in the current study, in-cylinder conditions are such that two distinct phases of ignition delay of pure n-heptane are not apparent (Figs. 3 and 5b); this was also observed in the RCM measurements of Di Sante [17] at compression temperatures in excess of 800 K. This is not unexpected as for n-alkanes the region of NTC is generally considered to end at approximately 750 K [41]; at the SOI for all tests of the toluene/n-heptane mixtures, the calculated in-cylinder global temperature was 775 K or greater.

As such the 2nd ignition delay visible for mixtures containing more than 25% toluene is unlikely to be attributable the NTC of the n-heptane present (Figs. 3 and 5b). Considering now those mixtures with 25% or less toluene, the effect of toluene is to increase the ignition delay period but not induce a 2nd ignition delay. At low temperatures, toluene can be oxidised via the abstraction of an H from the methyl group by O_2 , or preferentially non-selective OH radicals [12,18].



(1)



In the binary mixtures considered, the only source of OH radicals is those produced by H abstraction from n-heptane by O₂ (Eq. (3)), which is the first step in the radical branching process of internal isomerisation and peroxidation that governs the ignition chemistry of long alkyl chains [42].



The benzyl radicals that are formed in Eqs. (1) and (2) are thermally stable below 1000 K and cannot be oxidised further by O₂ [41]. Therefore, as previously suggested [12,18], it can be seen that toluene will delay the SOC by consuming radicals that otherwise would be utilised in the radical propagating reactions of n-heptane. This is confirmed by the use of the radical providing additive 2 EHN to equalise the ignition delay of binary mixtures containing differing proportions of toluene (Fig. 4). A second possible mechanism by which toluene may be acting as an inhibitor of radical branching during ignition delay is the physical presence of the non-reactive molecules within the fuel mixture. It is tentatively suggested that in addition to consuming radicals, the toluene molecules act as a diluent of the more reactive n-heptane molecules and thus reduce rates of reaction.

Figures 26a and b show the calculated in-cylinder global temperature profiles of the toluene/n-heptane binary mixtures at constant injection and constant ignition timing. At both timing conditions it can be seen that for all mixtures temperatures do not rise significantly above 800 K until sometime after SOC, when a substantial amount of heat release has occurred (Fig. 3). Therefore, it would seem that for those binary mixtures that do exhibit

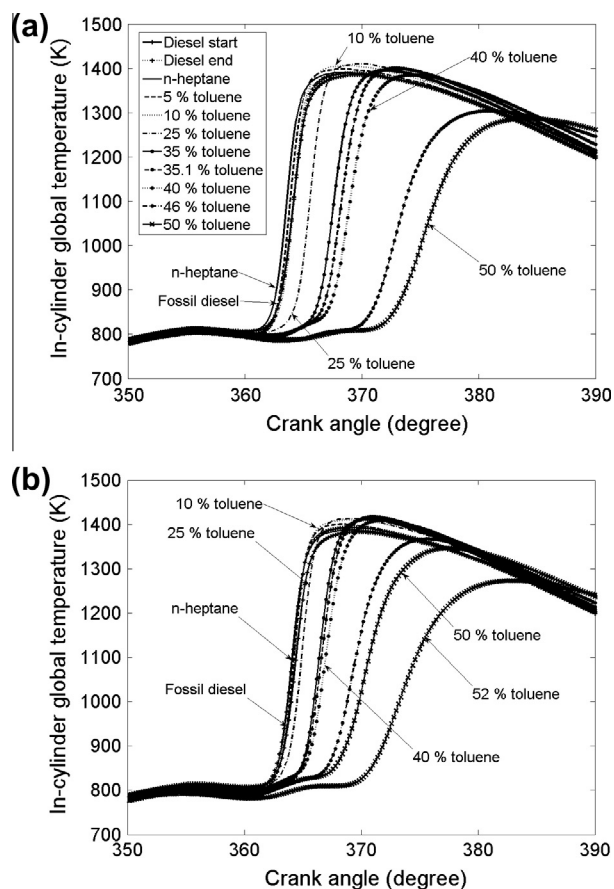


Fig. 26. Calculated in-cylinder global temperatures of toluene/n-heptane mixtures and reference fossil diesel at (a) constant injection and (b) constant ignition timing.

a 2nd ignition delay, thermal conditions are broadly the same as during the first period of ignition delay and so the initial reactions of the fuel components according to Eqs. (1)–(3) are likely to remain valid. As such, the following hypothesis is put forward regarding the presence of a 2nd ignition delay for those binary mixtures containing greater than 25% toluene.

At the point of SOC, local temperatures will have reached 900–1000 K and H₂O₂, formed by the radical branching reactions initiated by Eq. (3), will decompose and release large numbers of OH radicals, resulting in rapid branching reactions and ignition [42]. For the mixtures containing up to 25% toluene, the ensuing heat release from the local SOC is sufficient to initiate ignition throughout the charge. In the case of the mixtures containing more than 25% toluene, after ignition and consumption of a portion of the charge a further period of time is required during which a further build up of radical numbers must be occurring. The presence of toluene may prevent the escalation of ignition by removing OH from the radical pool produced by the decomposition of H₂O₂. Additionally, where ignition could be expected to spread to other areas of the fuel and mixture as stoichiometry allows [43], toluene may have prevented the build-up of sufficient radicals for this despite an increase in local temperature provided by the initial period of heat release (Fig. 3). During the 2nd ignition delay period, radical branching reactions involving n-heptane (Eq. (3)) and radical stabilizing reactions involving toluene (Eqs. (1) and (2)) continue. Fuel and air mixing would also continue and, given that a degree of pre-mixing has already occurred during the initial period of ignition delay, it could be expected that more of the fuel and air mixture would be at ideal stoichiometry for combustion at SOC2; it is also likely that local temperatures are somewhat higher as a result of the first heat release period. Thus this 2nd point of ignition is able to propagate throughout the cylinder charge. It is also possible during the 2nd ignition delay and SOC2 that the radical stabilising effect of toluene is potentially somewhat diminished as some toluene molecules will have been oxidised to thermally stable benzyl radicals during the 1st period of ignition delay.

It can be seen that the 2nd ignition delay period (Fig. 4b) increases as the toluene content of the binary mixture rises from 35% to 50%, and it follows that this can be attributed to fewer n-heptane molecules to produce radicals and more toluene to consume those that are produced. Ignition cannot occur at all for mixtures containing more than 52% toluene (at the conditions tested), indicating that at this point there is insufficient build up of radicals and local temperatures for any ignition to take place, regardless of the degree of fuel and air premixing.

4.2. Effect of 1-octene on low temperature behavior of 1-octene/n-octane binary mixtures

In contrast to the binary mixtures of toluene and n-heptane, those of 1-octene and n-octane show a reasonably linear relationship between ignition delay and the mixture composition (Fig. 16a). As the ignition delay is proportional to the 1-octene content, it is suggested that the longer ignition delays of the binary mixtures relative to n-octane can be attributed to the lower ignition quality of 1-octene (Table 2). A previous study [26] in which several alkanes and alkenes (including n-octane, 1-octene and 1,7-octadiene) were compared as pure fuel components, found that the ignition delay of an alkene relative to that of n-alkane of equivalent carbon chain length correlated highly with the percentage of double bonds present within the alkene. A similar relationship can be observed in the current study when considering that as the level of 1-octene increases in the binary mixtures, the proportion of double bonds do so also.

This implies that the addition of the 1-octene to the binary mixture does not result in significant interactions between those

molecules and the n-octane within the mixture. This is not a surprising result as the low temperature reactivity of alkenes is considered to be dominated by the saturated portions of the molecule [20,22,24], which will follow the same low temperature branching pathways as n-alkanes.

5. Conclusions

1. Increasing the percentage of toluene present in a binary mixture with n-heptane significantly reduces the ignition quality of a blend. Furthermore, at the conditions tested, n-heptane displayed one stage ignition but addition of more than 25% (wt/wt) of toluene resulted in two distinct ignition stages. Where the level of toluene present exceeded 50%, no ignition occurred whatsoever.
2. Where the toluene/n-heptane mixtures show only one stage of ignition delay and this increases in duration with the percentage of toluene present, this can be attributed to the radical stabilizing behavior of toluene. This effect can be offset by the radical proving additive 2 EHN.
3. Where two stages of ignition delay were apparent in the combustion of the toluene/n-heptane binary mixtures, the failure of the initial ignition to propagate throughout the cylinder charge can also be attributed to the radical consumption of toluene. It is suggested that the 2nd point of ignition is able to propagate throughout the charge as the second period of ignition delay allows for more fuel and air mixture to reach combustible stoichiometry.
4. Increasing the content of 1-octene present in a binary mixture with n-octane results in a proportional increase in ignition delay.
5. Exhaust emissions produced by the binary mixtures of toluene/n-heptane and 1-octene/n-octane show a significant influence of the in-cylinder thermal conditions as dictated by the ignition delay time. In the case of both binary mixtures, within select size ranges, an influence of stoichiometry on the number of particulars present in the exhaust gas is also apparent.
6. With the ignition delay of the binary mixtures removed as a variable, an increase in toluene or 1-octene content results in higher NO_x levels and can likely be attributed to a simultaneous rise in adiabatic flame temperature.

The hypotheses presented regarding the two stage ignition of the toluene/n-heptane mixtures may well be furthered with coupled CFD and chemical kinetics analysis, and the authors would welcome the use of the extensive experimental dataset acquired to test and validate CFD models and codes at the present experimental conditions.

Acknowledgments

The authors wish to thank BP Global Fuels Technology for financial and technological support, the UK Engineering and Physical Science Research Council also for financial support and Mr. Mart Magi for the droplet size measurements.

References

- [1] D.J. Wuebbles, A.K. Jain, *Fuel Process. Technol.* 71 (2001) 99–119.
- [2] European Union, in: Euro 5 and Euro 6 standards: reduction of pollutant emissions from light vehicles, 2010.
- [3] O. Badr, S.D. Probert, *Appl. Energy* 44 (1993) 197–231.
- [4] S. Tanaka, F. Ayala, J.C. Keck, J.B. Heywood, *Combust. Flame* 132 (2003) 219–239.
- [5] F. Contino, F. Foucher, C. Mounaim-Rousselle, H. Jeanmart, *Energy Fuels* 25 (2011) 1497–1503.
- [6] S. Zhong, M.L. Wyszynski, A. Megaritis, D. Yap, SAE Technical Paper 2005-01-3733, 2005.
- [7] J.A. Melero, M.M. Clavero, G. Calleja, A. Garcia, R.ü. Miravalles, T. Galindo, *Energy Fuels*, 2009.
- [8] A.B. Ross, P. Biller, M.L. Kubacki, H. Li, A. Lea-Langton, J.M. Jones, *Fuel* 89 (2010) 2234–2243.
- [9] J. Herzler, M. Fikri, K. Hitzbleck, R. Starke, C. Schulz, P. Roth, G.T. Kalghatgi, *Combust. Flame* 149 (2007) 25–31.
- [10] H.K. Ciezki, G. Adomeit, *Combust. Flame* 93 (1993) 421–433.
- [11] M. Hartmann, I. Gushterova, M. Fikri, C. Schulz, R. Schießl, U. Maas, *Combust. Flame* 158 (2011) 172–178.
- [12] J. Andrae, D. Johansson, P. Bjornbom, P. Risberg, G. Kalghatgi, *Combust. Flame* 140 (2005) 267–286.
- [13] J.C.G. Andrae, P. Bjornbom, R.F. Cracknell, G.T. Kalghatgi, *Combust. Flame* 149 (2007) 2–24.
- [14] J.C.G. Andrae, T. Brinck, G.T. Kalghatgi, *Combust. Flame* 155 (2008) 696–712.
- [15] C.V. Naik, W.J. Pitz, C.K. Westbrook, M. Sjöberg, J.E. Dec, J. Orme, H.J. Curran, J.M. Simmie, SAE Technical Paper 2005-01-3741, 2005.
- [16] J.M. Anderlohr, R. Bounaceur, A. Pires Da Cruz, F. Battin-Leclerc, *Combust. Flame* 156 (2009) 505–521.
- [17] R. Di Sante, *Combust. Flame* 159 (2012) 55–63.
- [18] G. Vanhove, G. Petit, R. Minetti, *Combust. Flame* 145 (2006) 521–532.
- [19] Z. Xiao, N. Ladommatos, H. Zhao, *Proc. Inst. Mech. Eng. D: J. Autom. Eng.* 214 (2000) 307–332.
- [20] R. Bounaceur, V. Warth, B. Sirjean, P.A. Glaude, R. Fournet, F. Battin-Leclerc, *Proc. Combust. Inst.* 32 (2009) 387–394.
- [21] S.K. Prabhu, R.K. Bhat, D.L. Miller, N.P. Cernansky, *Combust. Flame* 104 (1996) 377–390.
- [22] M. Mehl, G. Vanhove, W.J. Pitz, E. Ranzi, *Combust. Flame* 155 (2008) 756–772.
- [23] M. Mehl, W.J. Pitz, C.K. Westbrook, K. Yasunaga, C. Conroy, H.J. Curran, in: *Autoignition Behavior of Unsaturated Hydrocarbons in the Low and High Temperature Regions*, 2011, pp. 201–208.
- [24] P. Hellier, N. Ladommatos, R. Allan, S. Filip, J. Rogerson, *Fuel* 105 (2013) 477–489.
- [25] C.F. Cullis, A. Fish, J.F. Gibson, *Proc. R. Soc. Lond. Ser. A, Math. Phys. Sci.* 311 (1969) 253–266.
- [26] P. Hellier, N. Ladommatos, R. Allan, M. Payne, J. Rogerson, *SAE Int. J. Fuels Lubric.* 5 (2011) 106–122.
- [27] A. Schönborn, N. Ladommatos, J. Williams, R. Allan, J. Rogerson, SAE Technical Paper Series 2007-24-0125, 2007.
- [28] P. Patel, R. Balachandran, N. Ladommatos, P. Richards, SAE Technical Paper 2011-01-1836, 2011.
- [29] G.A. Ban-Weiss, J.Y. Chen, B.A. Buchholz, R.W. Dibble, *Fuel Process. Technol.* 88 (2007) 659–667.
- [30] A. Schönborn, N. Ladommatos, J. Williams, R. Allan, J. Rogerson, *Combust. Flame* 156 (2009) 1396–1412.
- [31] J.P. Szybist, A.L. Boehman, J.D. Taylor, R.L. McCormick, *Fuel Process. Technol.* 86 (2005) 1109–1126.
- [32] C.J. Mueller, A.L. Boehman, G.C. Martin, SAE Technical Paper Series 2009-01-1792, 2009.
- [33] S. Turns, *An Introduction to Combustion: Concepts and Applications*, McGraw Hill, 2000.
- [34] M.V. Roux, M. Temprado, J.S. Chickos, Y. Nagano, *J. Phys. Chem. Ref. Data* 37 (2008) 1855–1996.
- [35] E.W. Prosen, F.D. Rossini, *J. Res. Natl. Bureau Standards* 38 (1945) 263–267.
- [36] D.R. Tree, K.I. Svensson, *Prog. Energy Combust. Sci.* 33 (2007) 272–309.
- [37] N. Ladommatos, P. Rubenstein, P. Bennett, *Fuel* 75 (1996) 114–124.
- [38] A. Alexiou, A. Williams, *Fuel* 74 (1995) 153–158.
- [39] J.D. Rockenfeller, F.D. Rossini, *J. Phys. Chem.* 65 (1961) 267–272.
- [40] J.F. Griffiths, P.A. Halford-Maw, D.J. Rose, *Combust. Flame* 95 (1993) 291–306.
- [41] M.J. Pilling, *Low-Temperature Combustion and Autoignition*, Elsevier, 1997.
- [42] C.K. Westbrook, *Proc. Combust. Inst.* 28 (2000) 1563–1577.
- [43] J.E. Dec, SAE Tech. Paper Ser. (1997) 970873.